Carbon diffusion in Iron A kinetic Activation-Relaxation Technique Study

Normand Mousseau

Université de Montréal

Vancouver, August 2017

In collaboration with

Gerard Barkema (Utrecht)
Charlotte Becquart (Lille)
Laurent Karim Béland (Oak Ridge)
Othmane Bouhali (TAMUQ)
Peter Brommer (Warwick)
Fadwa El-Mellouhi (QEERI)
Simon Gelin (UdeM)
Anne Hémeryck (Toulouse)
Antoine Jay (Toulouse)
Jean-François Joly (Ottawa)
Gawonou Kokou N'tsouaglo (UdeM)
Laurent Lewis (UdeM)
Eduardo Machado-Charry (CÉA)
Sami Mahmoud (UdeM)
Pascal Pochet (CÉA)
Oscar Restrepo (UdeM)
Nicolas Richard (CÉA)
Mickaël Trochet (UdeM)

With the support of

Natural Science and Engineering Research Council of Canada (NSERC)
Fonds de recherche du Québec - Nature et technologies
Canada Research Chair Foundation
Canadian Foundation for Innovation
Fondation NanoScience (Grenoble)
Qatar National Research Fund
Université de Montréal

Computer Time : Calcul Québec / Compute Canada

Kinetics of disordered systems

How do glasses relax at low T?

What are the defects?

What is the impact of impurities (e.g.: H in Si)

How do we understand the Si/SiO_2 interface?

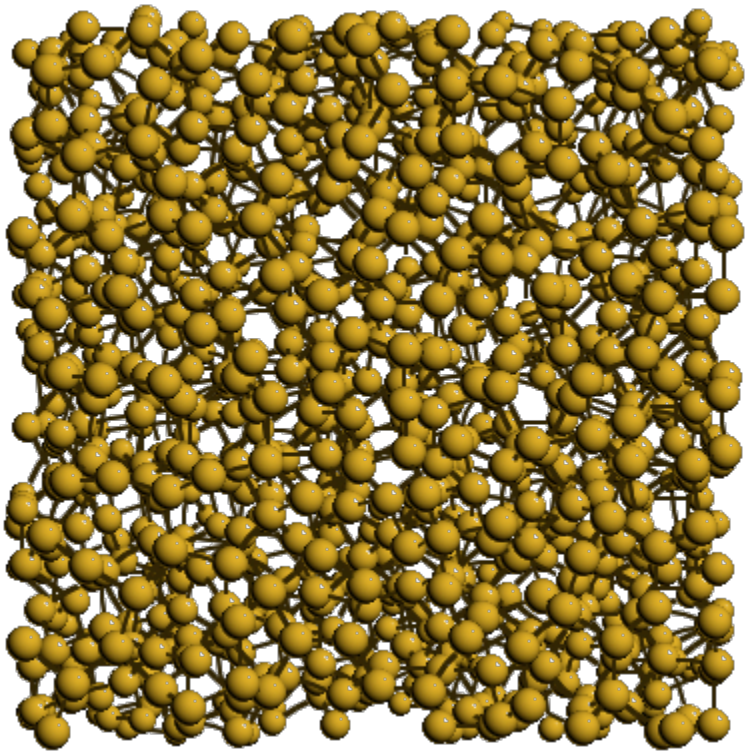

How does ciment microstructure evolve?

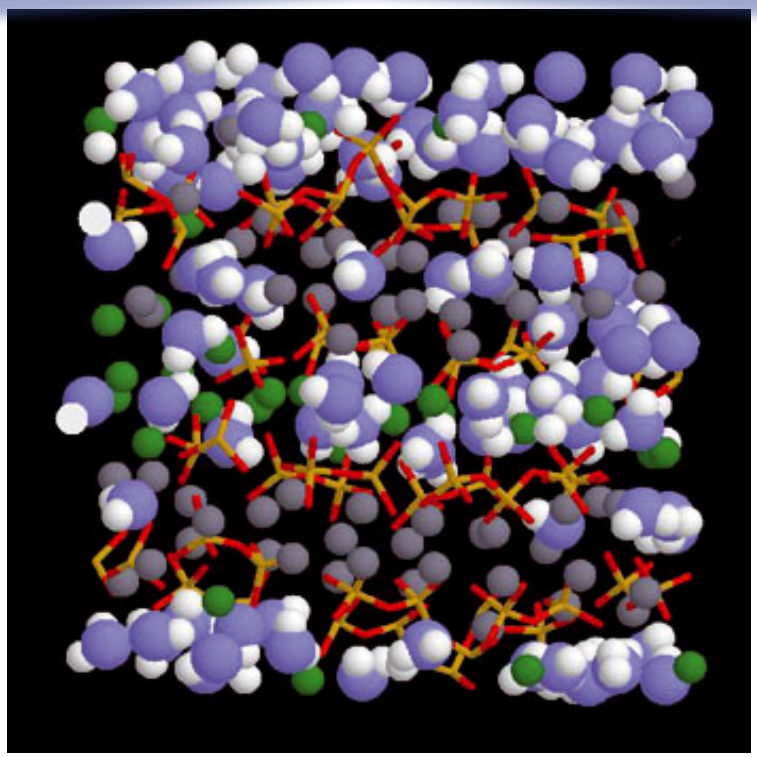

R. Pellenq

Energy landscapes

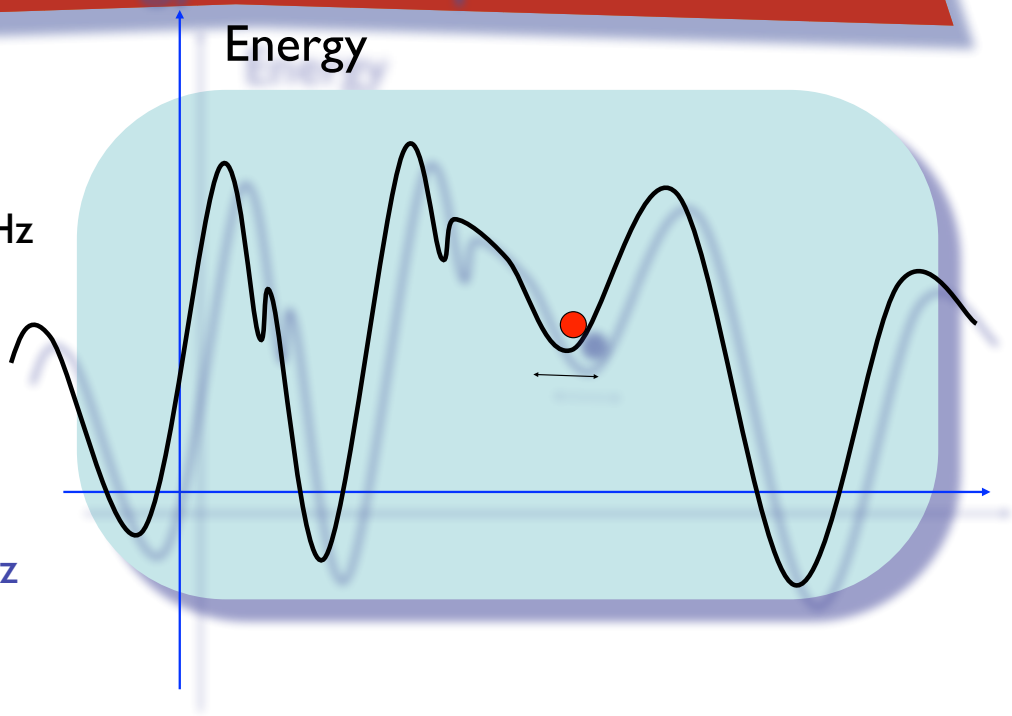

Atoms vibrate at 10^{12} Hz

Rare events (activated events) occur at 10^{6} Hz or less

Generic problem:

How to explore the space of variables of a high dimensional cost function?

TST : activated dynamics

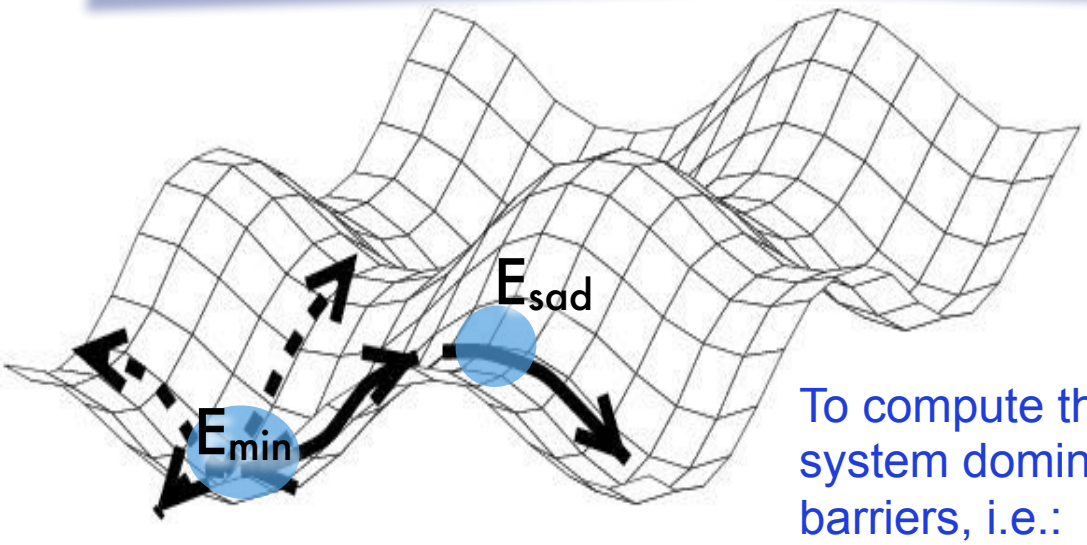

$$\Gamma = \Gamma_0 e^{-\Delta E / k_B T}$$

To compute the dynamics in a system dominated by activation barriers, i.e.:

1. Uncorrelated jumps
2. High barriers wrt $k_B T$

we need to know:

1. Knowledge of saddle points
2. Prefactor

Standard Kinetic Monte Carlo

In standard KMC, the problem studied must be defined on a lattice

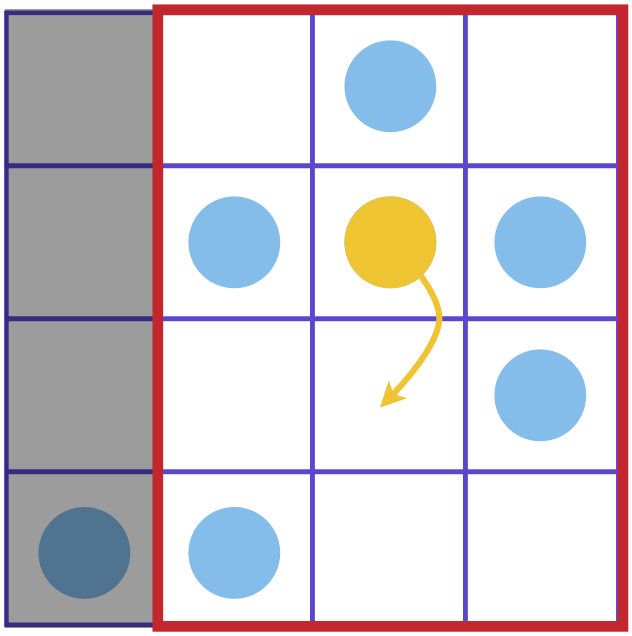

A. B. Bortz, M. H. Kalos, and
J. L. Lebowitz, J. Comput. Phys. (1975).

A list of events must then be constructed.

Including the final sites we get:

2^{10} = 1024 different events and barriers and prefactor

At a given moment, we select one of the possible events at random based on their rate *r of occurrence*

and make the move and update the clock according to

$$\Delta t = -\frac{\ln \mu}{\sum r_i}$$

Kinetic Monte Carlo simulation of the evolution of radiation damages in Fe

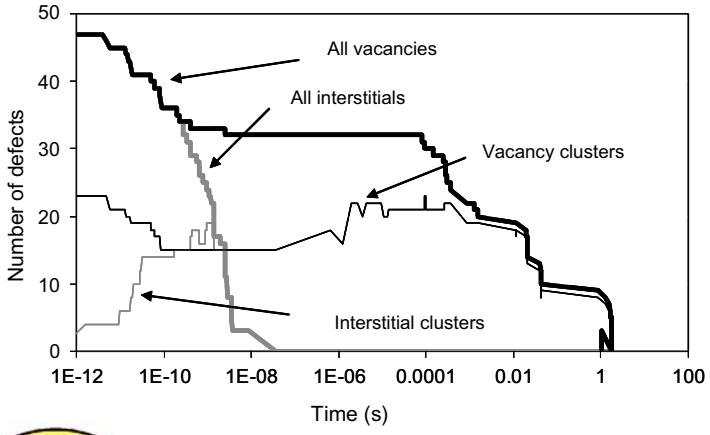

Different events included in the object-based catalog

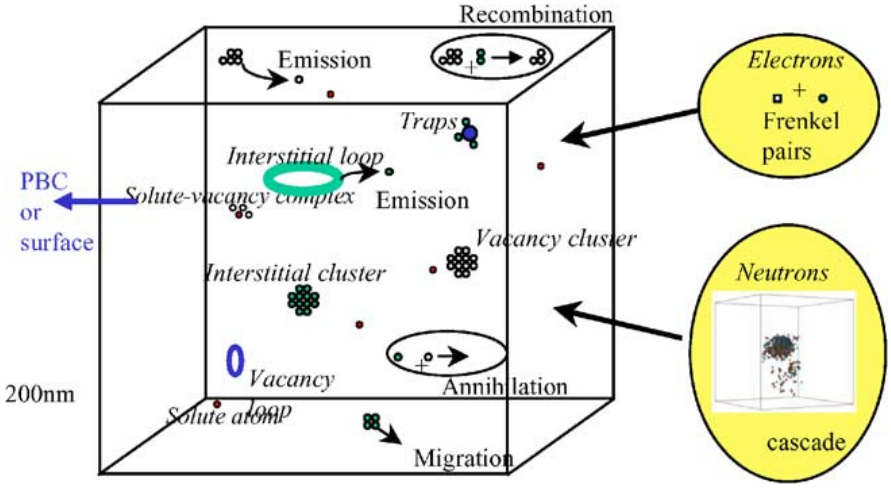

Example of a simulation at 600 K

C. Domain, C.S. Becquart & L. Malerba, J. Nucl. Mat. (2004)

Limitations of Standard Kinetic Monte Carlo

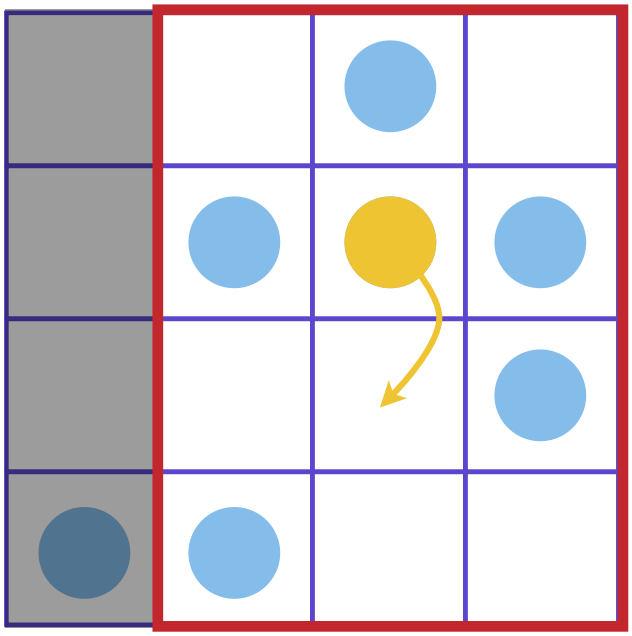

1. Uses a predefined and limited catalogue of known diffusions events and barriers at T=0

   can miss mechanisms

2. Constrains atoms to move only on a predefined lattice which can be real or effective

   atoms are not always on lattice

3. Supposes that there are no long-range interactions between defects

   elastic effects can be important

kMC with event list rebuilding at each step

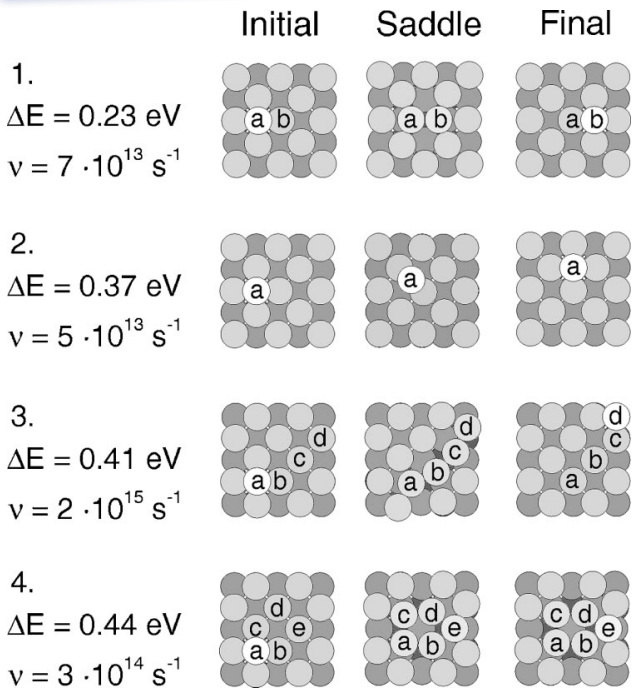

Henkelman and Jonsson, JCP 2001

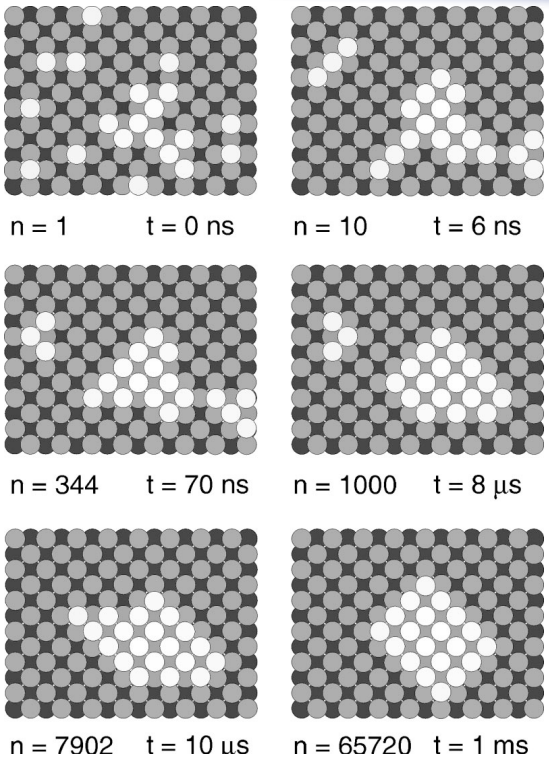

This method works well for small or simple systems. However, the number of barriers at each step much remain low.

Overcoming these limitations

Over the last few years, many methods have also tried to introduce a catalog with off-lattice configurations

Kinetic ART (El-Mellouhi, Lewis and Mousseau, PRB 2008)

- uses ART nouveau (currently, fastest saddle-point search method)
- Topological classification, handles any complexity and full elastic effects

Self-Learning KMC (Kara, Trushin, Yildirim and Rahman, JPCM 2009)

- limited saddle point searching capacities (drag + repulsive bias potential)
- pattern recognition based on the existence of a lattice (no elastic effects)

Self-evolving atomistic KMC (Xu, Osetsky and Stoller, PRB 2011)

- uses dimer method
- new searches in local environment (no elastic effects)

Local-environment KMC (Konwar, Bhute and Chatterjee, JCP 2011)

- NEB for predetermined mechanisms (biased catalog)
- Local geometrical classification (no elastic effects)

KINETIC ART

Can we recover the dynamics of relatively complex systems dominated by activated diffusion?

Kinetic ART

1) Generates the catalog and refines events with

ART nouveau

2) Classifies and reconstructs events with

Topological analysis - NAUTY

3) Evolves the system with

Kinetic Monte Carlo

Finding barriers with ART nouveau

The activation-relaxation technique is defined in three steps.

1) Leave the harmonic basin;
   threshold determined by value of lowest curvature

2) Push the configuration up along the corresponding direction;
   energy is minimized in the perpendicular hyperplane;
   can converge to the saddle point with any desired precision

3) Minimize the energy;
   bring the configuration into a new minimum

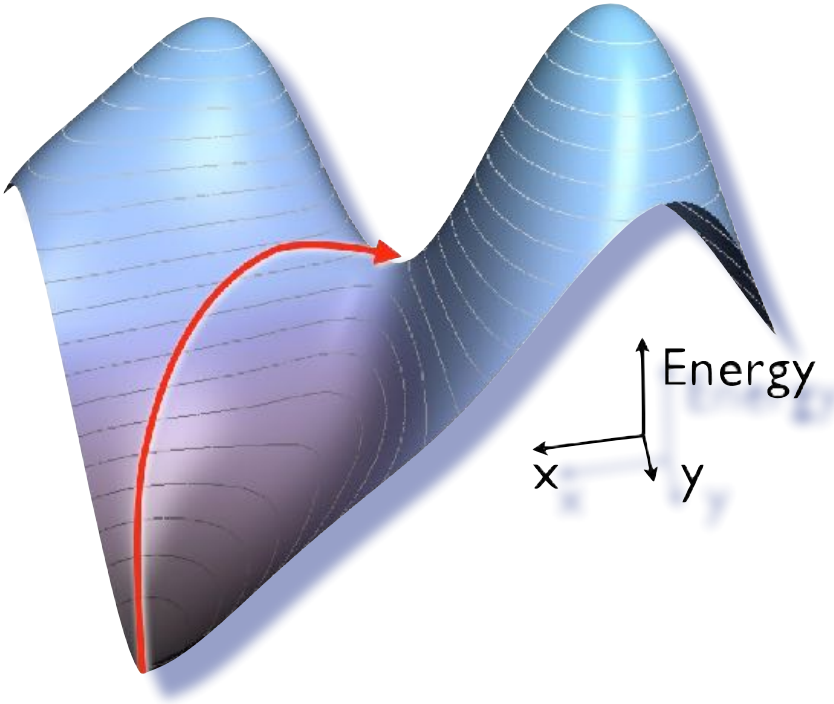

Barkema & Mousseau, Phys. Rev. Lett. 77 (1996);
Malek & Mousseau, Phys. Rev. E 62 (2000);

Generating an event

ART nouveau can be used to identify barriers

1. Start from a local minimum

2. Select the atom in the center of the local topological region; displace this atom and its neighbours slowly.

3. Follow this direction until an eigenvalue become negative.

4. Push along the corresponding eigenvector until total force is zero. (Saddle point)

5. Converge to a new minimum (event).

6. Assign the event to the atom that has moved most.

7. Repeat, from (2) a desired number of times.

8. Move to the next atom and start at (2)

Features of ART

not sensitive to the real space complexity of activated jump nor the height of the activation energy barrier, which can be very high

not biased toward pre-determined mechanisms

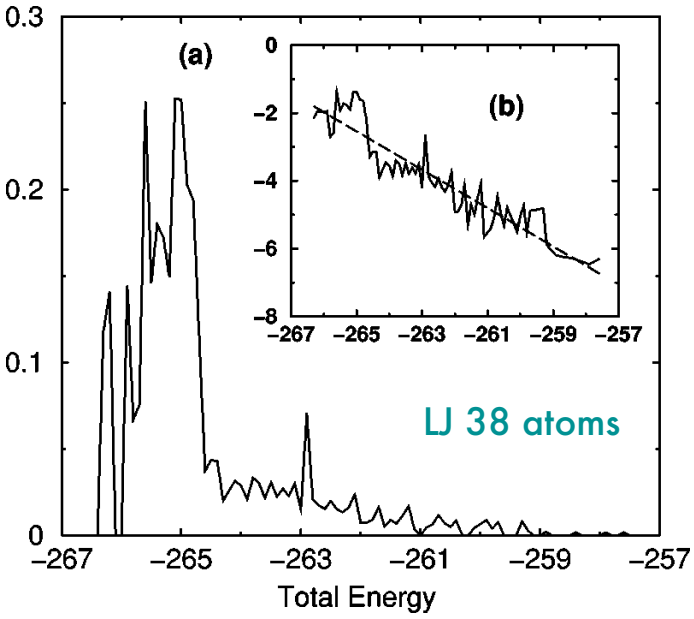

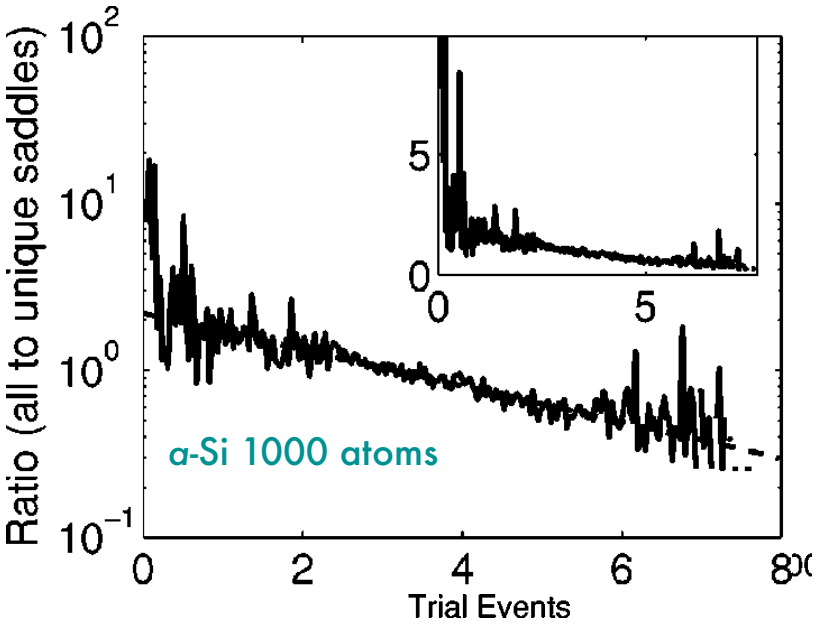

very efficient numerically

seems to sample all classes of events (ergodic)

events are reversible

Comparison with other methods

Algo.	ART nouveau				ARTn (Olsen)		Dimer method		Improved dimer		GSM
Ref.					[33]				[34]	[35]	[6]
System	*a-Si*	V_{Si}	C_{20}	SiC	Pt(111)	Pt(111)	Pt(111)	Pt(111)	C_6H_{10}	PHBH/H_2O	VO_x/SiO_2
BC	Bulk	Bulk	Isol.e	Surf.	Surf.	Surf.	Surf.	Surf.	Isol.	Sol.	Isol.
Pot.	SW	DFT	DFT	DFT	Morse	Morse	Morse	Morse	DFT	QM/MM	DFT
Method		PBE	LDA	PBE					B3LYP	AM1	B3LYP
DOF	3000	12[1]	60	222[1]	3	525	3	525	48	144	12[1]
$\langle f \rangle$	235	210	322	262	145	372	204	335	384[2]	425[3]	330
$\langle f \rangle_s$	670	302	718	728	145	2163	204	2148	-	-	-
A/S	2.72	79/78	434/201	134/75	-	-	-	-	-	-	-

E Machado-Charry, LK Béland, D Caliste, L Genovese, NM and P Pochet, J. Chem Phys. **135**, 034102, 11 pp., (2011).

E Cances, F Legoll, M-C Marinica, F Minoukadeh, and F Willaime, J. Chem. Phys. **130**, 114711 (2009).

Nanocalorimetry measurements

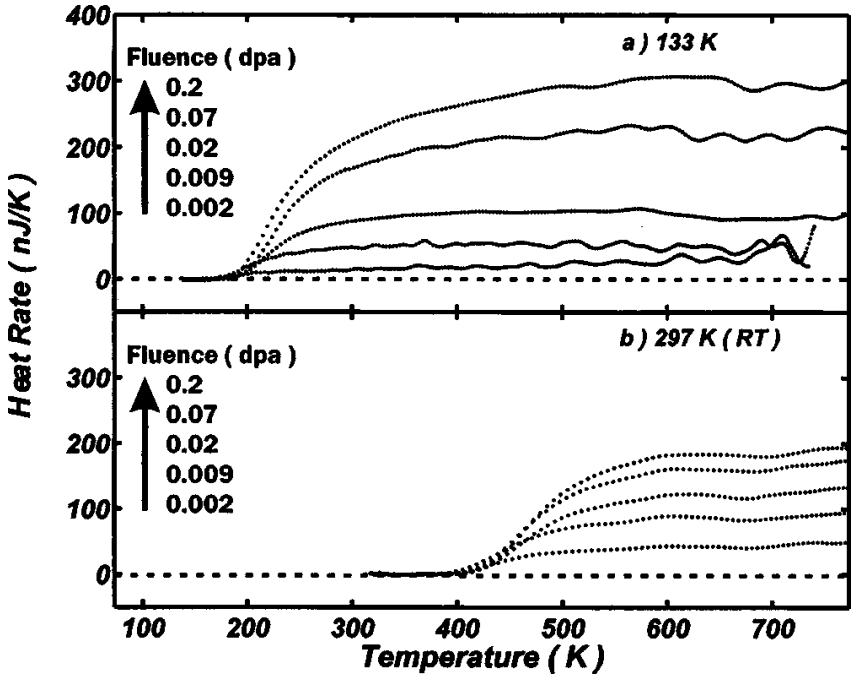

Heat release curves for different implantation fluences at

(a) 133K

(b) room temperature

Mercure et al. Phys. Rev. B 71, 134205 (2005)

Energy landscape of *a*-Si

1. How does the local energy landscape vary with relaxation ?
   i. use a 4000-atom model of amorphous silicon
   ii. start from a random assembly of atoms
   iii. use ART + modified Stillinger-Weber potential
2. Can we use these results to explain recent nanocalorimetry experiments ?
   i. start from a well-annealed thin sample of *a*-Si
   ii. implant it with Si atoms at low temperature
   iii. measure the heat released during heating

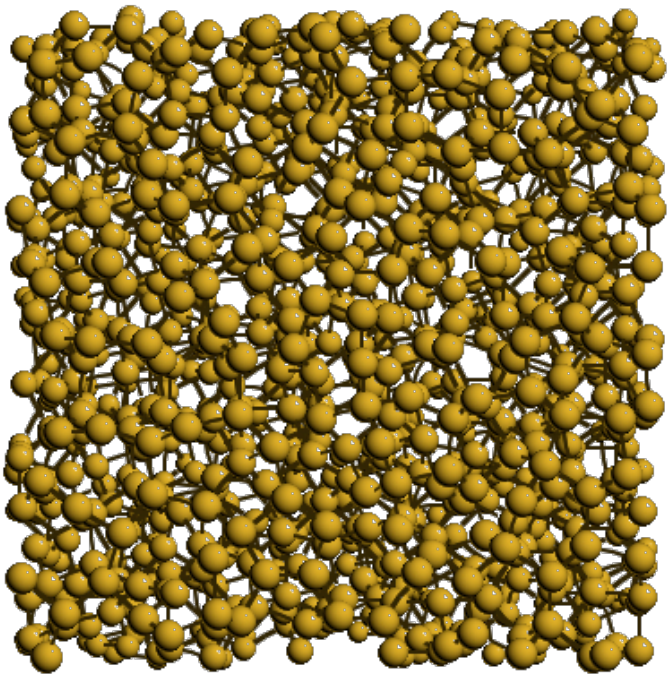

H. Kallel, N.M., F. Schiettekatte, PRL 105, 045503 (2010).

Relaxation and bond-defect concentration

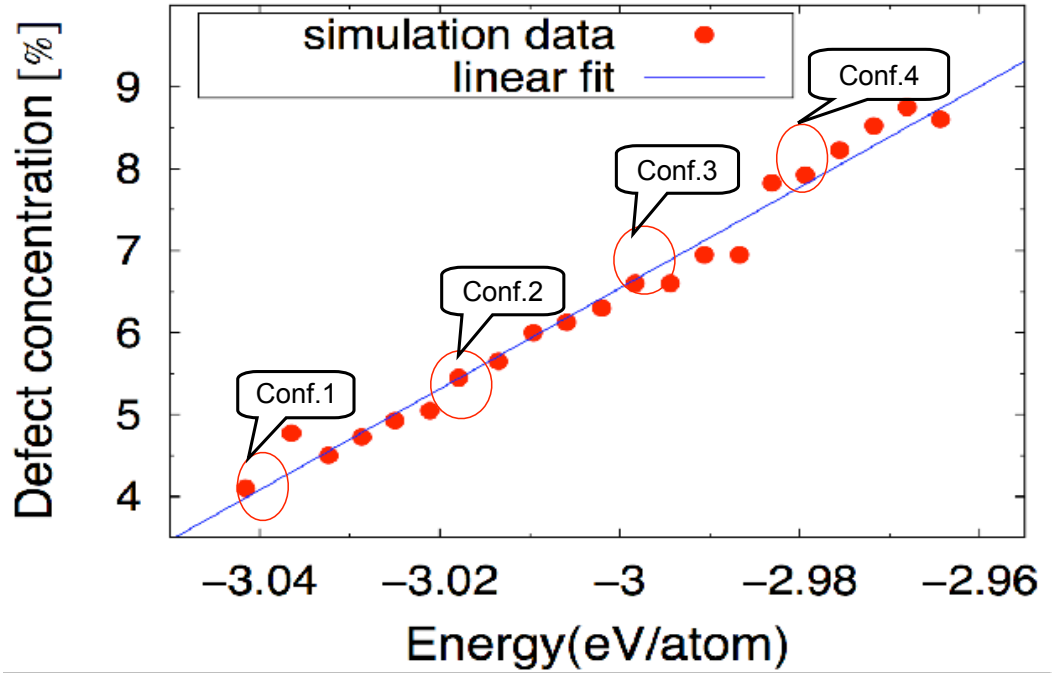

We select 4 configurations and generate 100 000 events around each of these leading to about 12000 *unique* events each.

A few definitions...

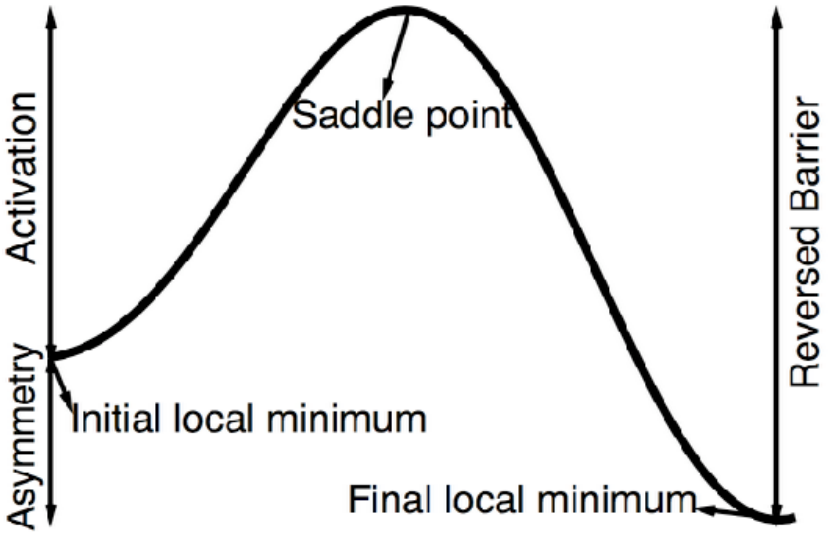

Activation (forward) barrier distribution

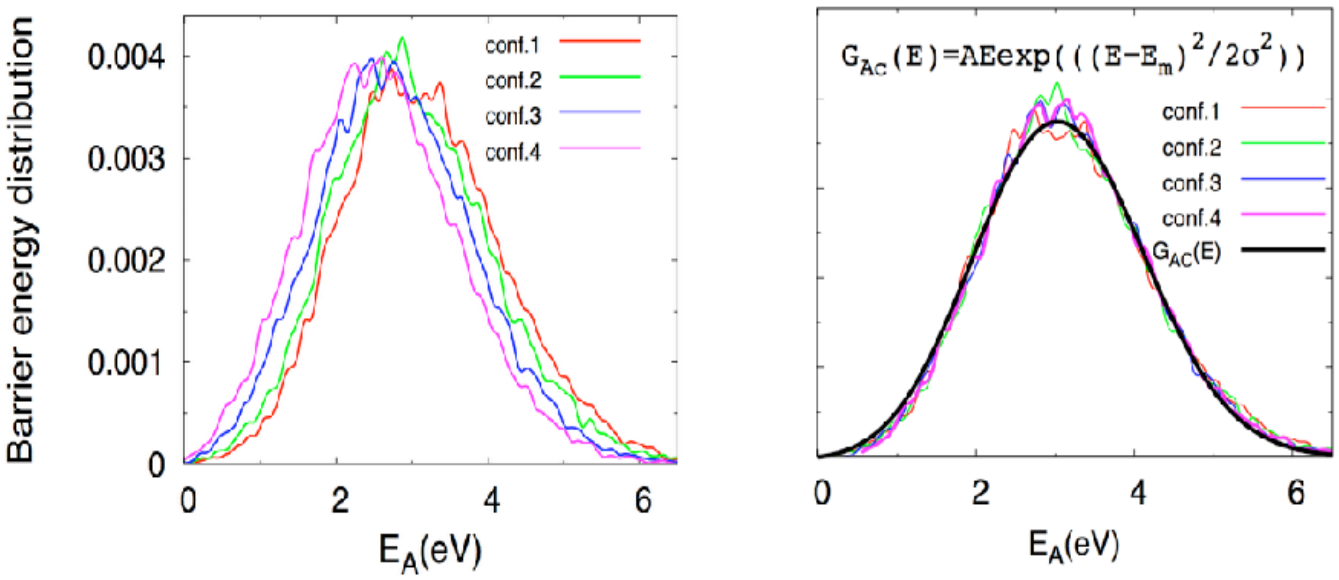

	Conf.1	Conf.2	Conf.3	Conf.4
$<E_{Ac}>$(eV)	3.157	3.005	2.793	2.603
ΔE_{Ac} (eV)	1.067	1.053	1.034	1.024

Reverse barrier distribution

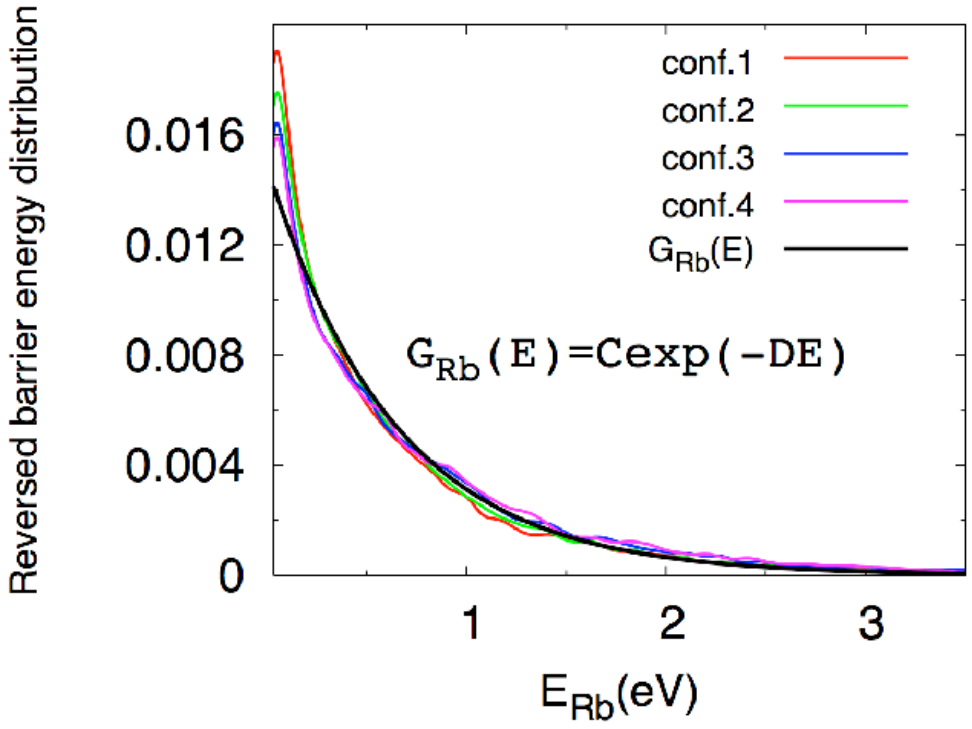

Reverse barrier distributions are ***independent*** of level of relaxation

Energy asymmetry

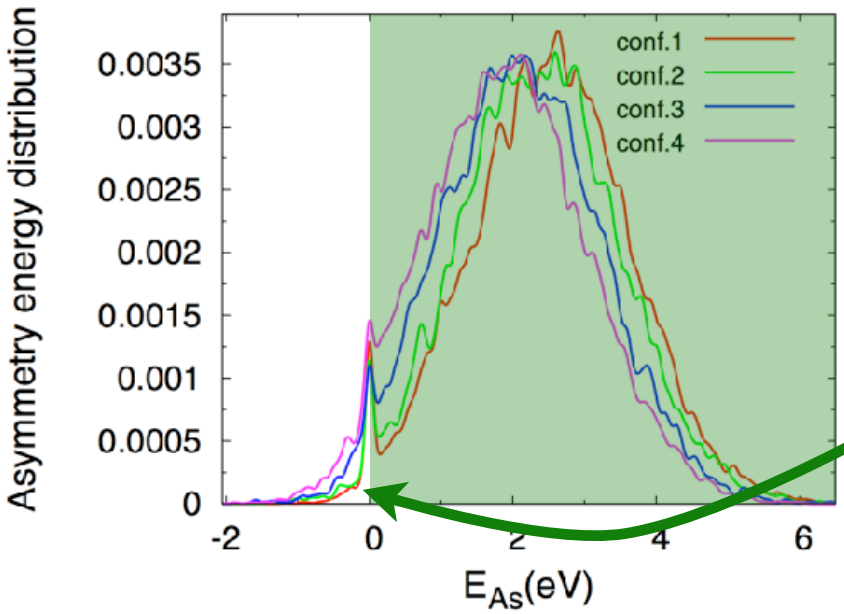

Only events with a final state lower than the initial matter.

1. ***Convolution*** of forward and reverse energy barrier distribution
2. The amount of the energy released decreases as the bond defects concentration decreases.

Nanocalorimetry measurements

Samples are implanted at low temperature and then heated, while heat released is measured, revealing a number of features:

1. the stored-strain, measured as the heat rate, saturates as a function of implantation fluence;
2. the heat flux released as the sample is heated is relatively uniform as a function of temperature, for temperatures ranging from 118 to 775 K;
3. for low fluences, the heat-rate follows nearly the same curve, irrespective of the implantation temperature. For fluences near saturation, the heat release amplitude increases with decreasing implantation temperature.

These results were explained by the presence of a continuous distribution of states where each annealing event releases an amount of heat independent of its activation energy.

Heat released vs Temperature

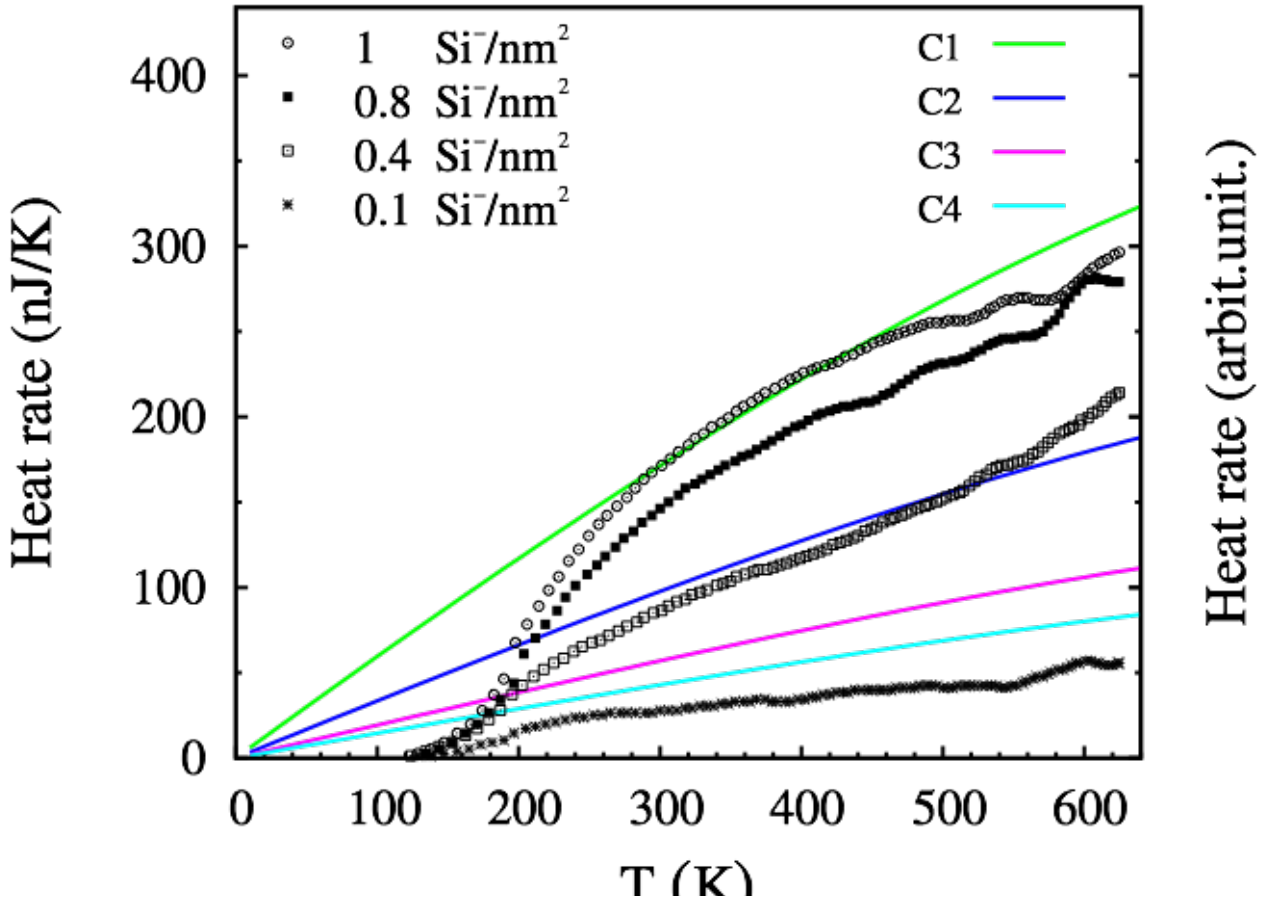

Conclusions

1. There is a linear relation between energy and coordination defects
2. The forward energy-barrier distribution shifts to higher energy with relaxation
    i. its shape is independent of the degree of relaxation
    ii. in agreement with the Vogel-Fülcher law
3. The reverse energy-barrier distribution is an exponential, **independent** of the degree of relaxation
4. Our simulation results explain heat released as a function of temperature observed in nano-calorimetry measurements
5. The energy landscape picture can therefore provide direct link to experiments

H. Kallel, N.M., F. Schiettekatte, PRL 105, 045503 (2010).

Some applications of ART nouveau

Ab initio calculation of defects diffusion mechanisms in Silicon, GaAs

El-Mellouhi and NM - PRB (2004, 2005), J. Appl. Phys.(2006); Malouin, PRB (2007)

Amorphous silicon - structure, relaxation and activated mechanisms

Barkema, Song, Malek, Kallel and NM - PRL (1996,1998, 2010), PRE (1998), PRB (2000, 2001,2003)

Amorphous gallium arsenide - structural properties

Lewis and NM - PRL (1997), PRB (1997), Barkema and NM, JPhys:CondMatt (2004)

Interstitials in Fe

M.-C. Marinica, F. Willaime and N. Mousseau, PRB (2011)

Silica glass - structural properties, activated mechanisms

Barkema, de Leeuw - NM - JCP (2000)

Lennard-Jones clusters and glasses

Brébec, Limoge, Malek and NM, PRB (2000), Def. Diff. Forum (2001)

Protein folding

Derreumaux, Wei and NM - J. Mol. Graph. (2001), JCP (2003), Proteins (2004);
St-Pierre, Derreumaux and NM (2008)

Protein aggregation

Boucher, Derreumaux, Melquiond, Santini and NM - JACS (2004), Biophys. J., Structure (2004), JCP (2005), Accounts Chem. Res.(2005), Proteins(2006), JCP (2006,2007)

A topological classification

We suppose that all configurations can be classified in terms of their topology and that the events generated will have the same topological evolution.

1. Using the neighbour list, a graph is generated
2. The graph is analysed at its topology identified
3. All graphs with the same topology belong to the same class

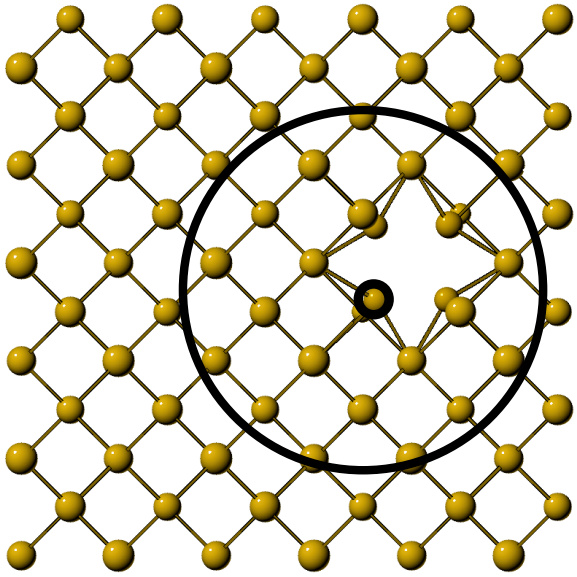

F. El-Mellouhi, NM and L.J. Lewis, PRB **78**, 153202 (2008).

NAUTY

NAUTY is a program for computing automorphic groups of graphs; it can also produce a canonical labelling taking into account symmetry operations of the graph.

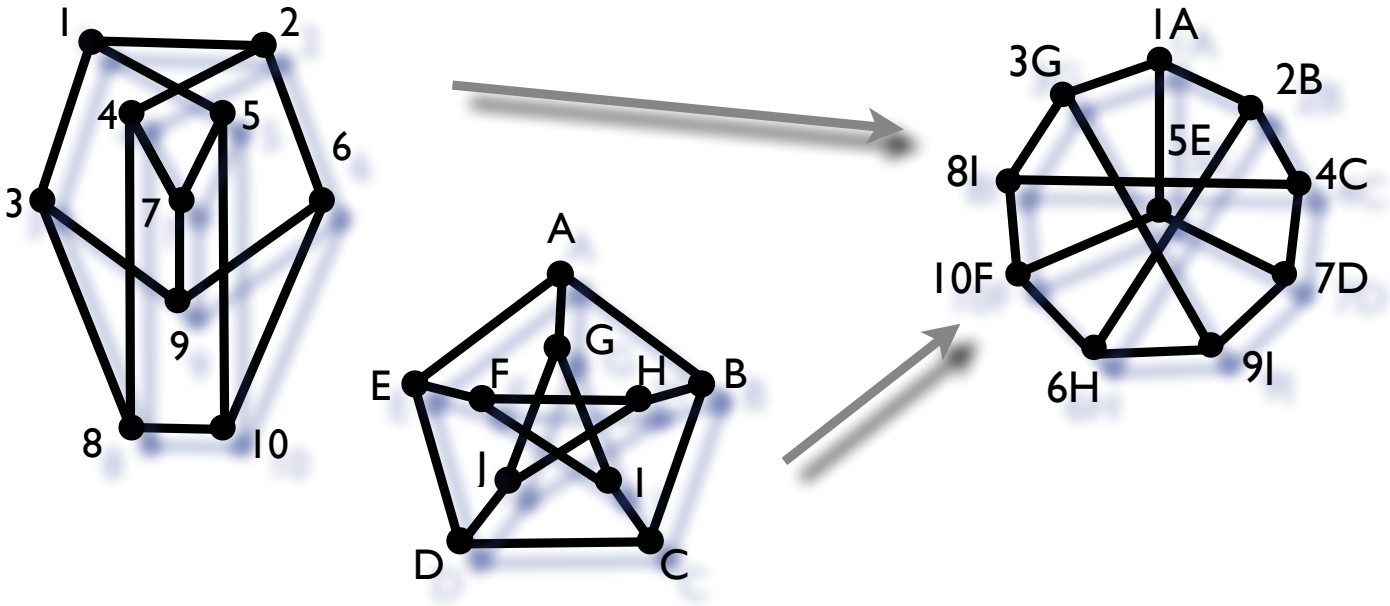

Brendan D. McKay, *Practical Graph Isomorphism*, Congressus Numerantium, **30** (1981) 45-87.
http://cs.anu.edu.au/~bdm/nauty/

Topological analysis with NAUTY

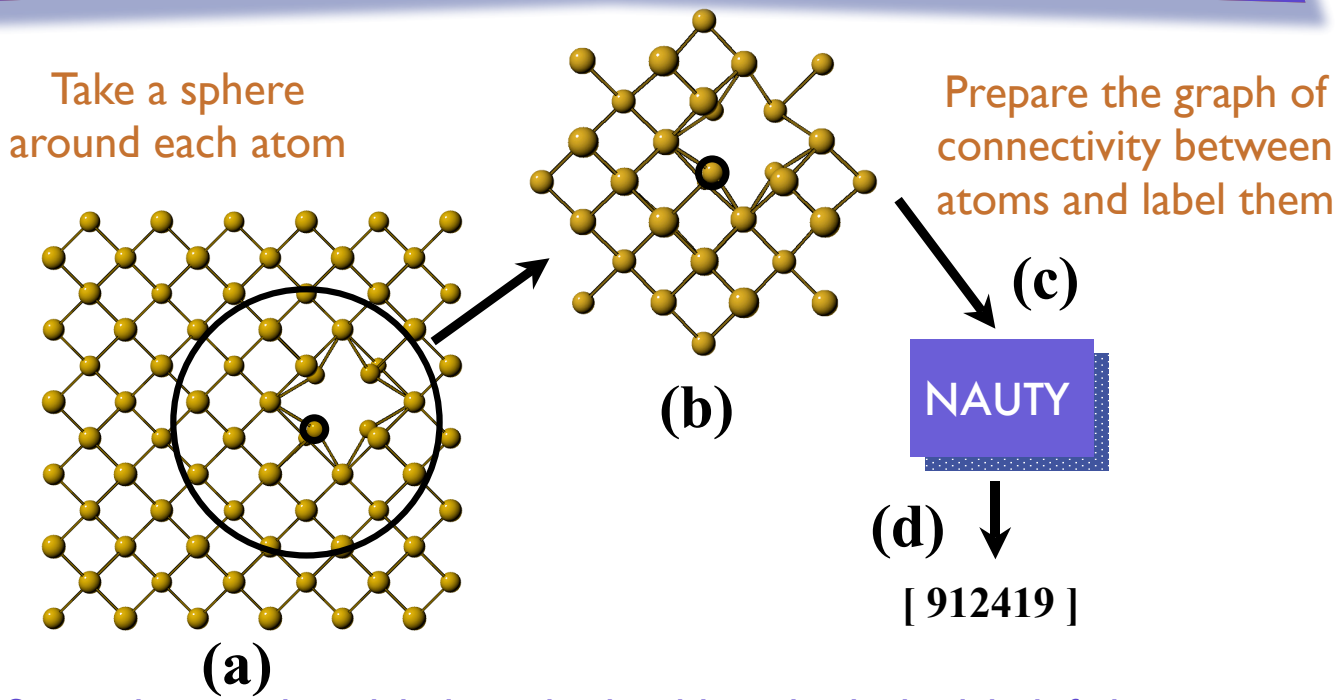

1. Store the topology label in a hash table, rehash the label if clustering occurs;
2. Update the occurrence of the topology;
3. If topology is completely new, store it and find the events and rate lists associated with it.

The algorithm

After an event :

1. The topology of all the atoms within the active part of the event is evaluated again;
2. If the topology is known, import the list of events; if not, generate ART events;
3. If some of the old topologies do not have enough events, try a few more ART steps;
4. Store these new topologies.
5. Relax all relevant barriers to take into account elastic effects
6. Compute rate and apply KMC

Taking into account long-range elastic effects

After each event, saddle points are refined and the energy barriers are reevaluated to take in to account short and long-range effects.

To decrease the costs, only events with low-barriers are refined. Those with a high barrier are given the default value associated with the init

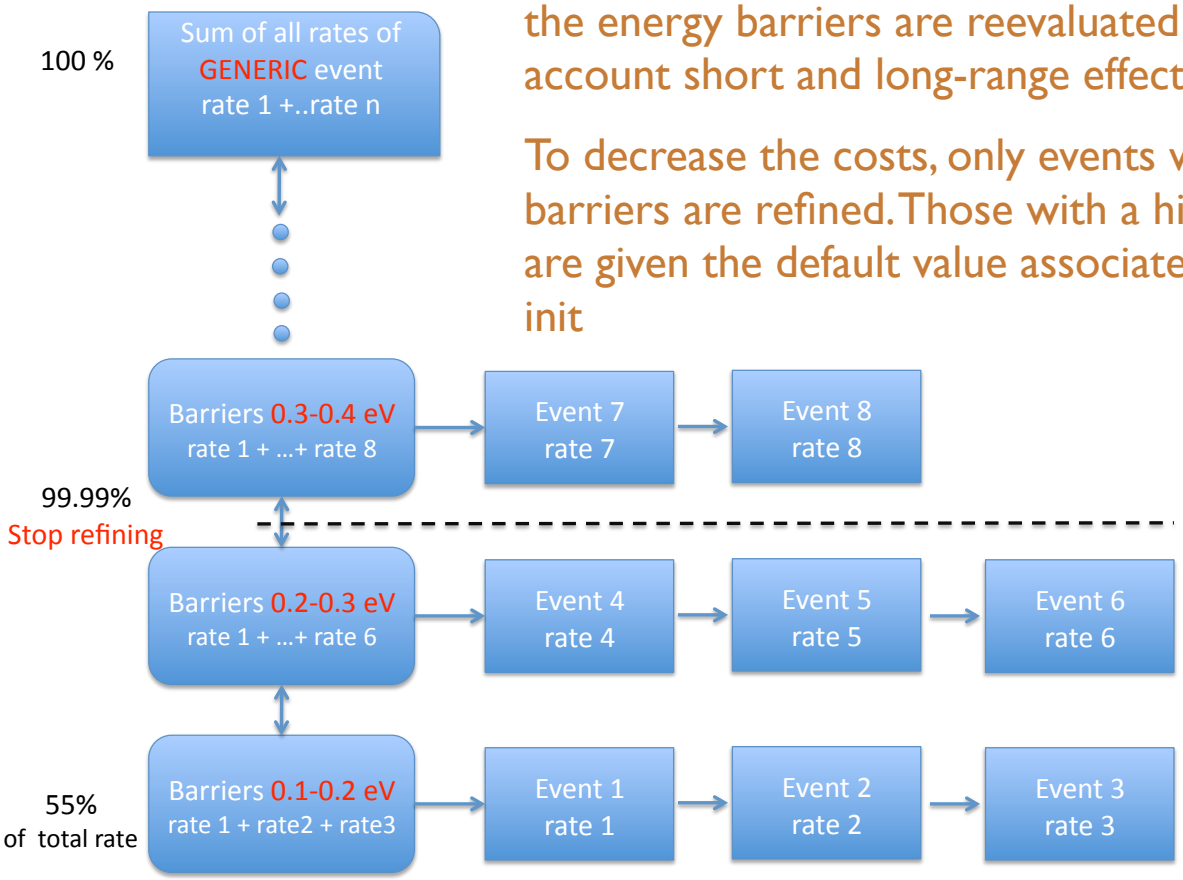

Taking care of low-energy barriers

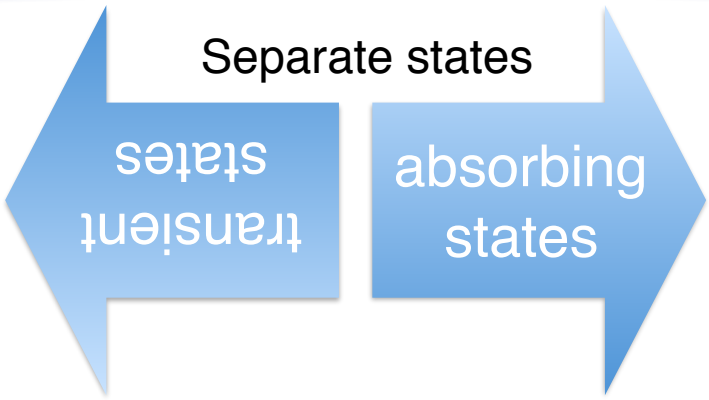

- low-energy barriers
- fast transitions between t.s.

- high-energy barriers

- final states: after some time the system will end up in a a.s.

The Mean Rate Method

Puchala et al., JCP **132**, 134104 (2010)
LK Béland, P Brommer, F El-Mellouhi, J-F Joly and NM, PRE **84**, 046704 (201

Application to amorphous silicon

1. What is the relation between average coordination (i.e. defects) and relaxation?
2. How do defects move?
3. No accelerated technique has been applied to these disordered materials

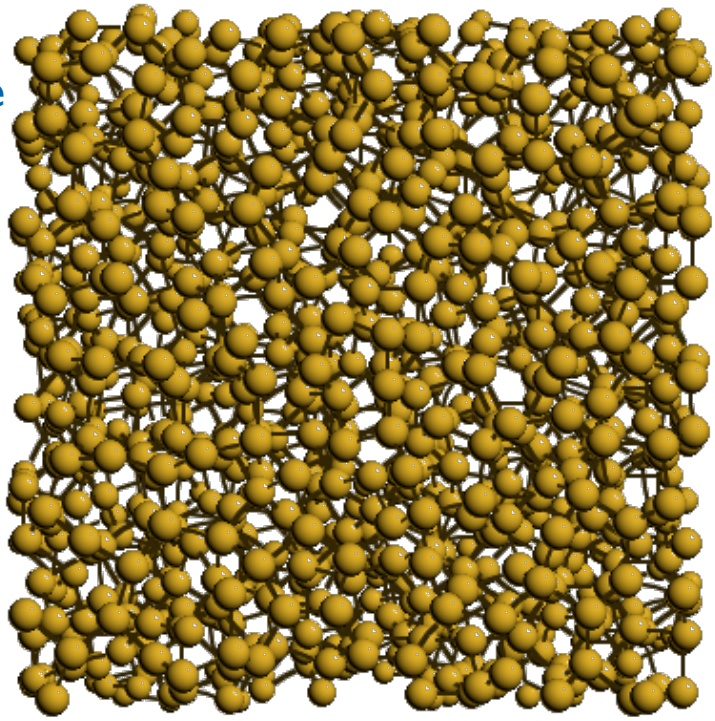

Joly *et al*, PRB 2013; PRB (submitted 2015)

Application to amorphous silicon

1000-atom box

modified Stillinger-Weber potential

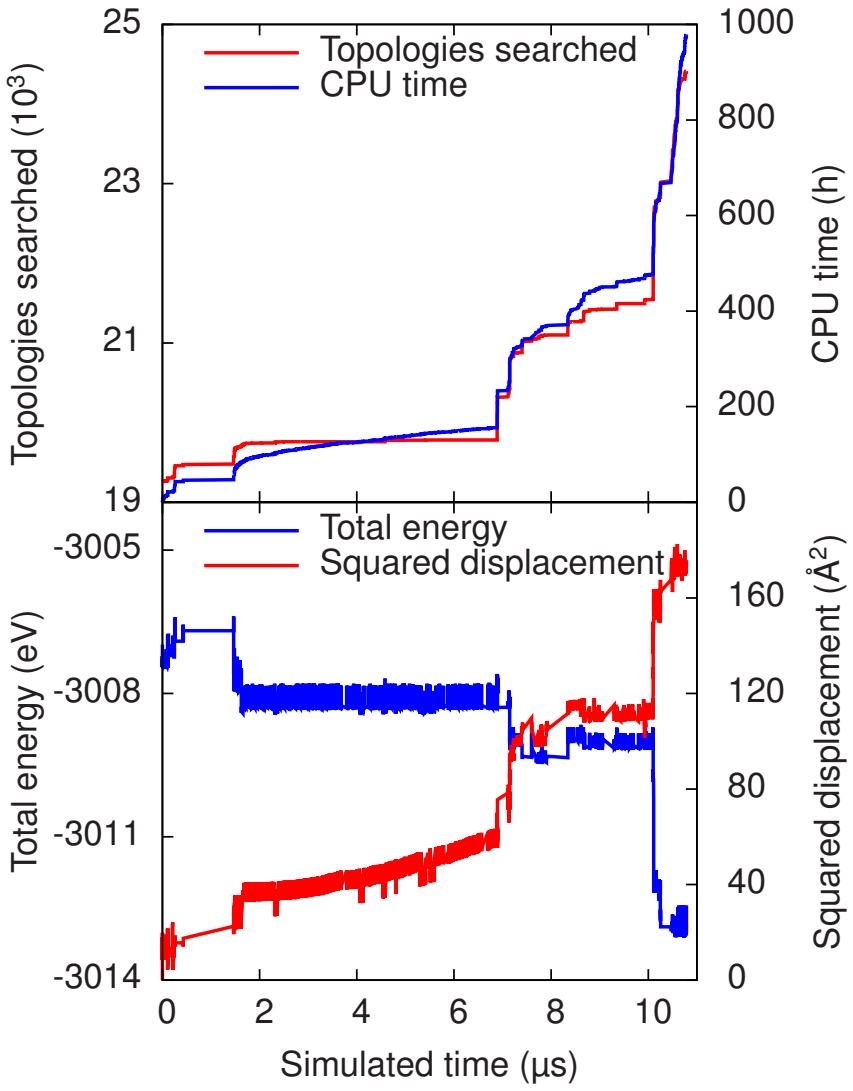

Stability of vacancies

999-atom box (1 vacancy)

modified Stillinger-Weber potential

T=300 K

Initial catalog: 32 120 events

E_{basin} = 0,45 eV

24 processors (Intel Westmere-EP).

Most vacancies disapear within 1 ns

Here, vacancy survives after 120 µs

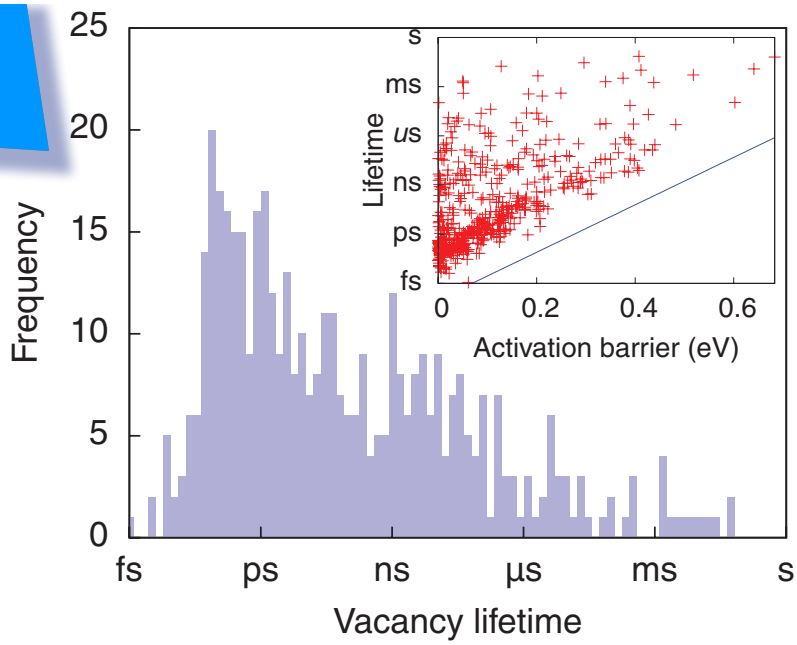

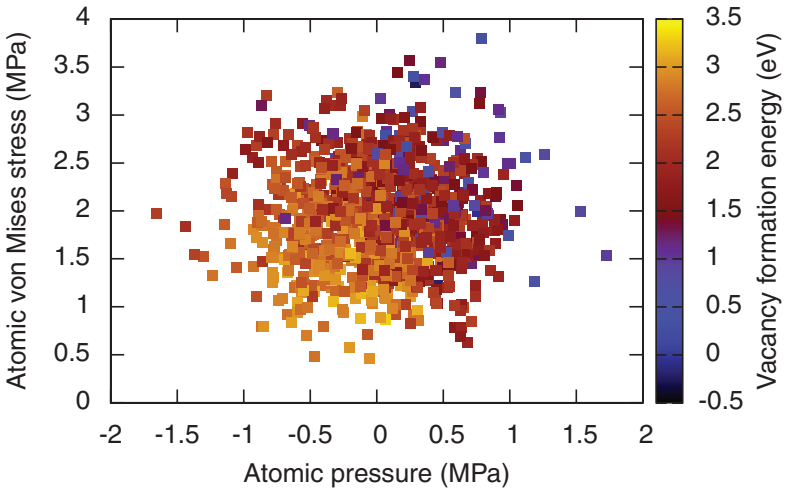

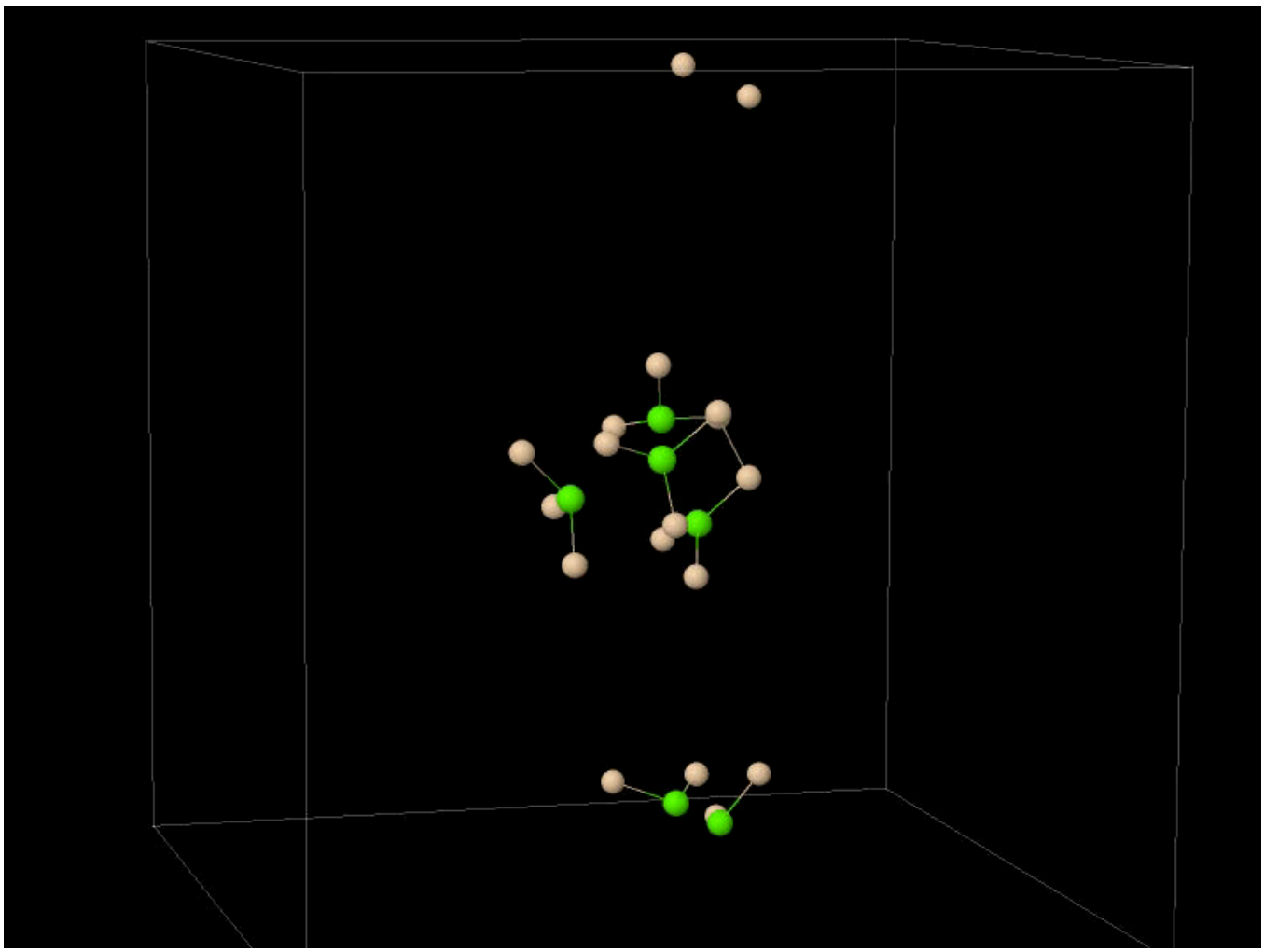

Other features

- Use the LAMMPS forcefield library
- Fixed prefactor (typically 10^{13} s^{-1})
- Handles flickers
- Handles alloys directly
- Parallelized for events and forcefield
- Order (1) force calculations
- Various capabilities at selecting events, species, etc.
- Flexible handling of boundary conditions, including surfaces

Si anneal after ion

27000 atoms box, 300 K, 1 atom implanted at 3 keV

1 ns simulated with MD, serves as initial configuration for kART run

Comparison with nanocalorimetry experiments is possible

Handling of low-barrier by basin mean-rate method makes these runs even faster

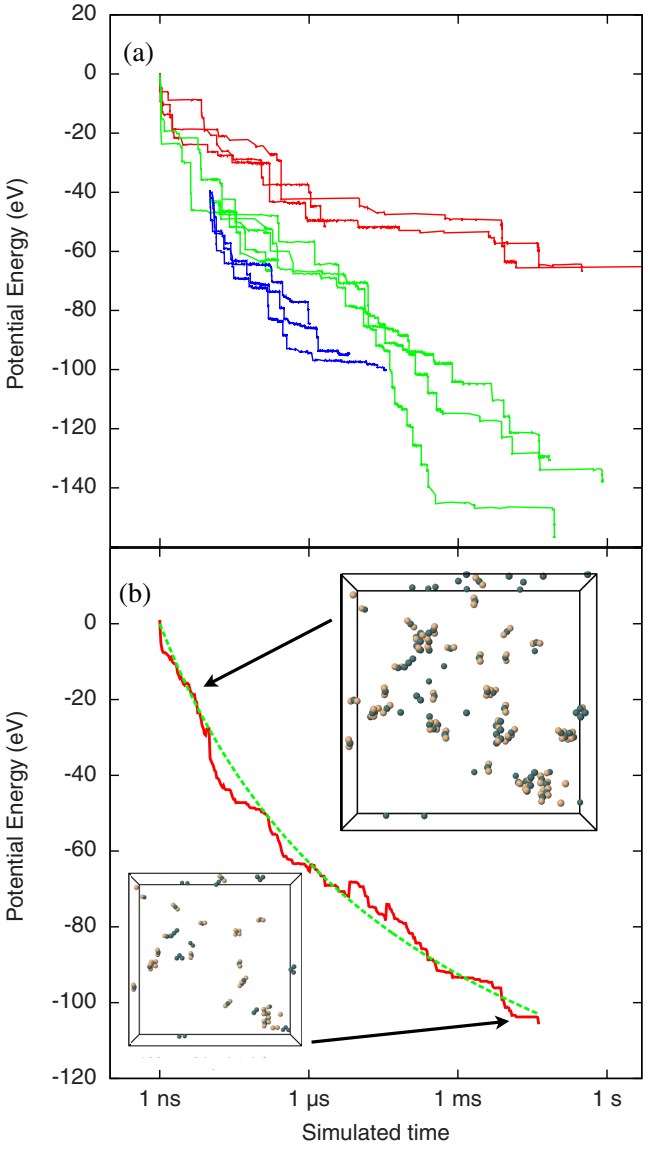

Béland et al, PRL 2013; PRB 2013

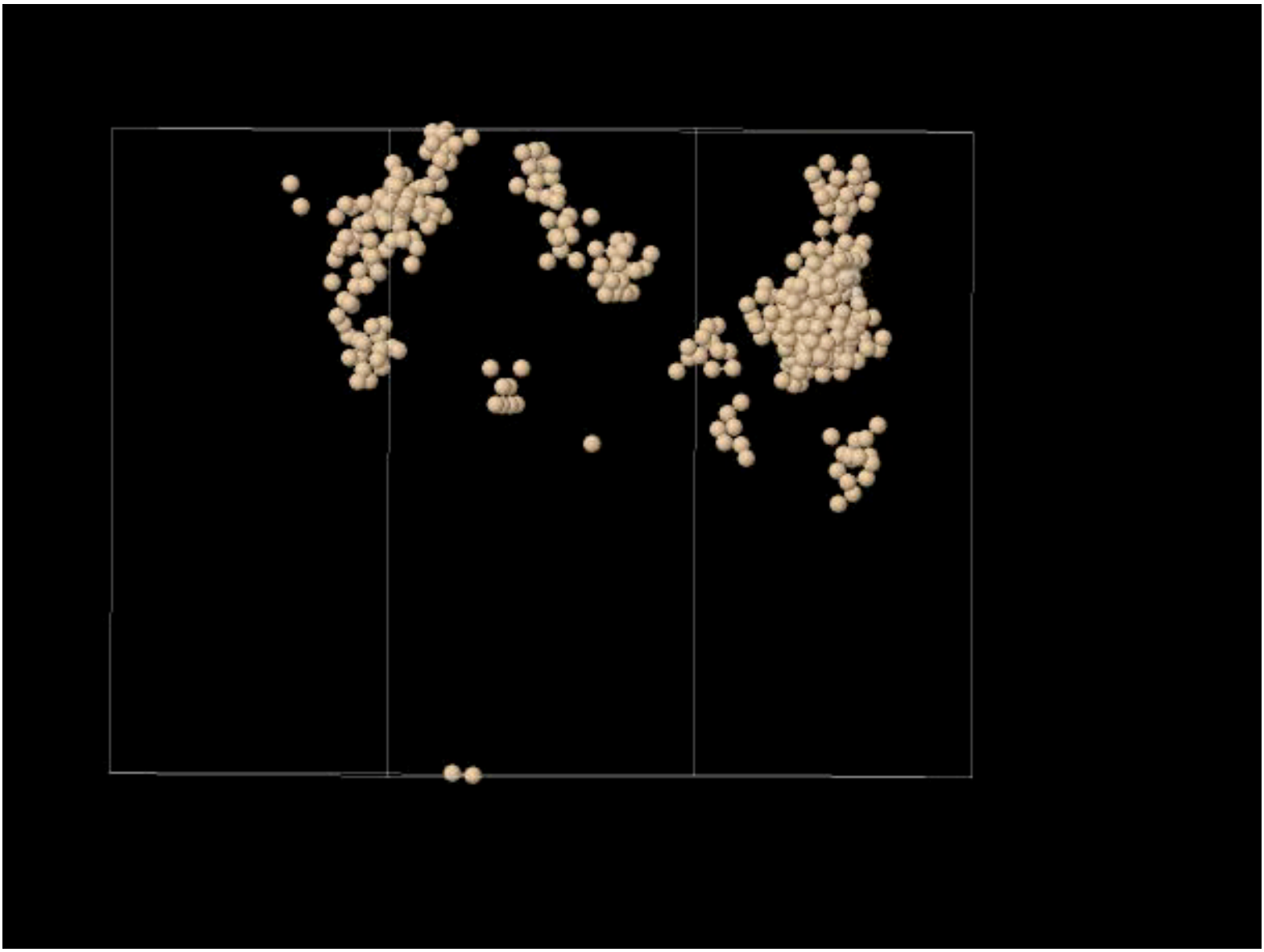

c-Si anneal after ion

The jumps in time are caused by the basin method acceleration.

A large number of topologies must be explored to describe the correct PES (potential energy surface) and kinetics.

We show that the damaged system can execute transitions with a quasi-continuum of energy barriers

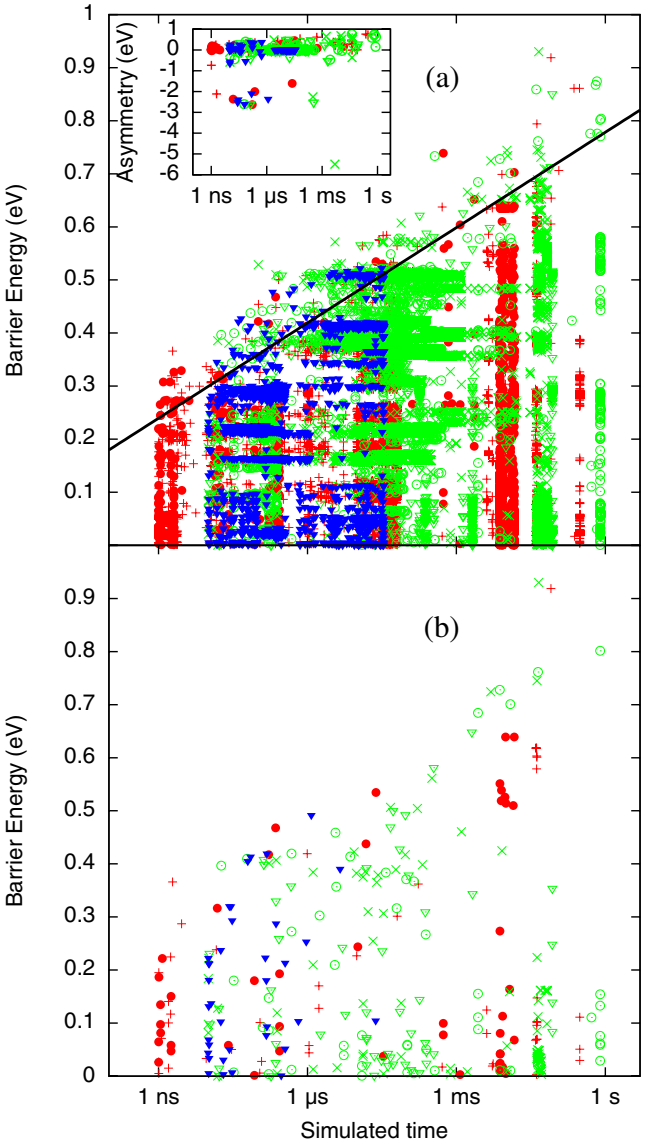

Nanocalorimetry measurements : *c*-Si

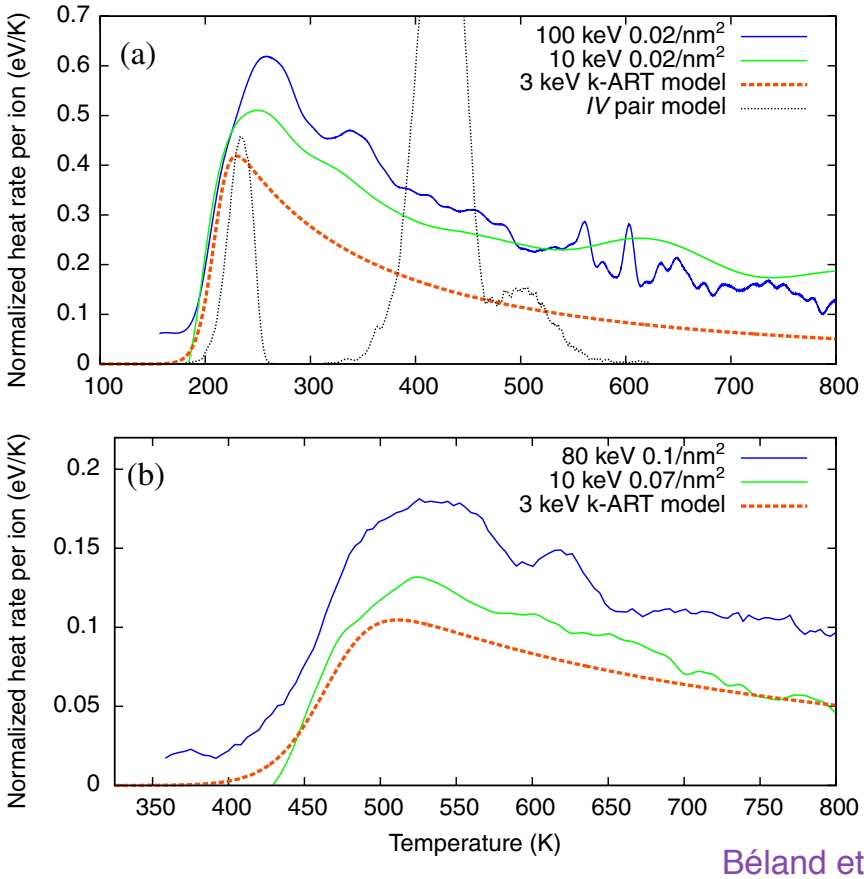

Béland et al, PRL 2013

Revisiting: understanding telegraph noise

With Antoine Jay, Mélanie Rayne, Anne Hémeryck, Vincent Goiffon, Nicolas Richard and Pierre Magnan

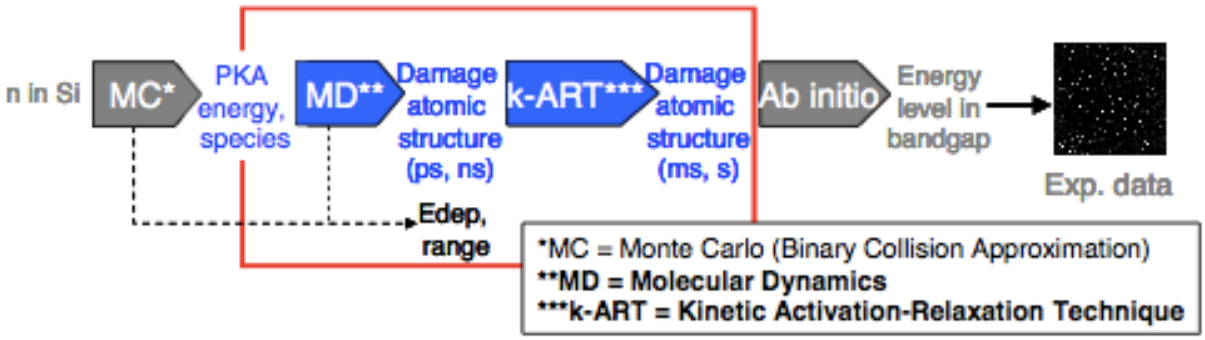

1. 1 million atoms initially
2. 10 to 100 keV
3. Relaxation first with MD (1 ns) then k-ART
4. Stillinger-Weber

Revisiting: understanding telegraph noise

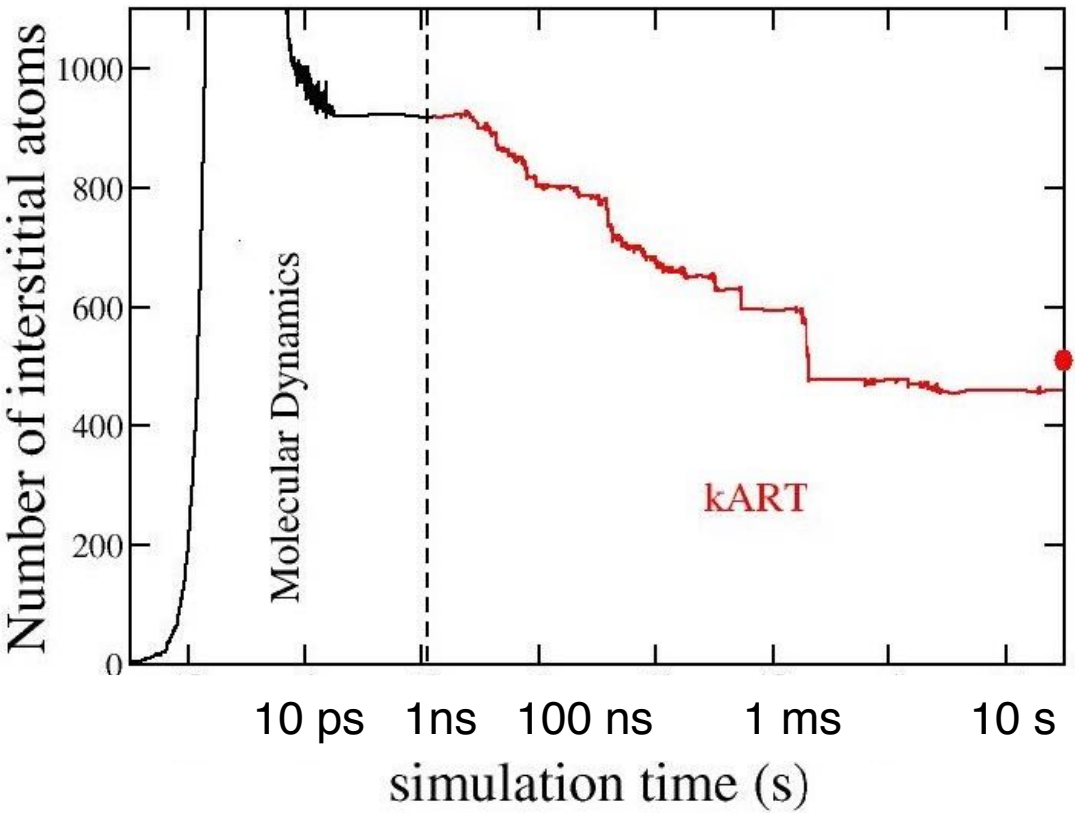

A possible candidate: a tri-interstitiel flicker

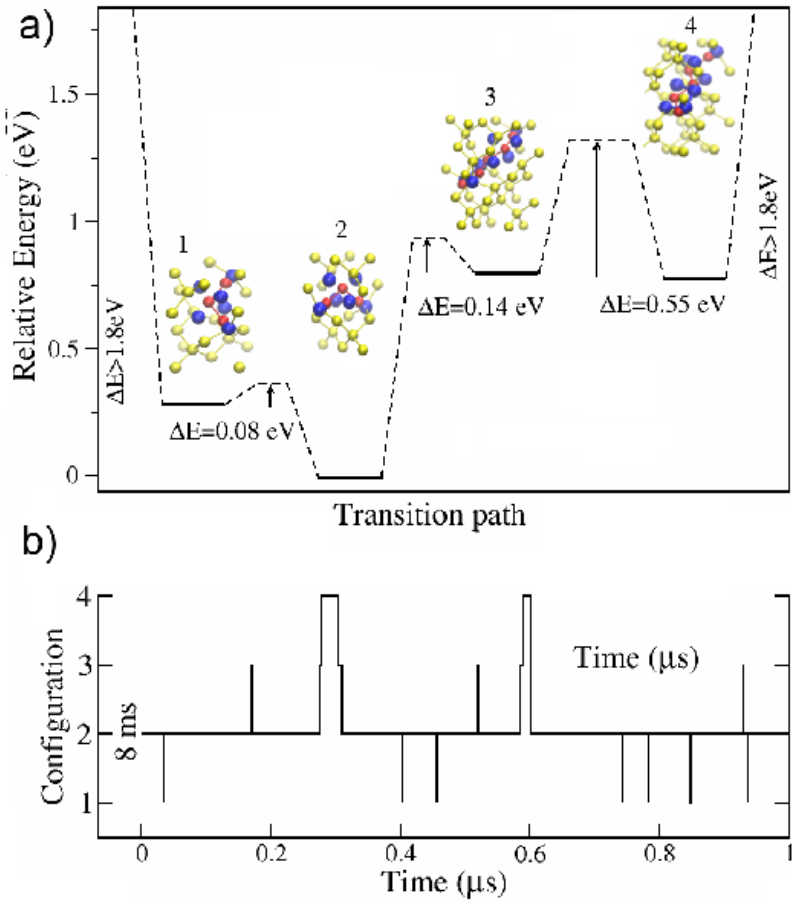

C diffusion in Fe

What are the fundamental mechanisms responsible for metal dusting ?

1. Use Becquart's C-Fe EAM potential
2. Start with simple defects :
   1. C interstitials
   2. C subsitutionals

a) Fe jumps

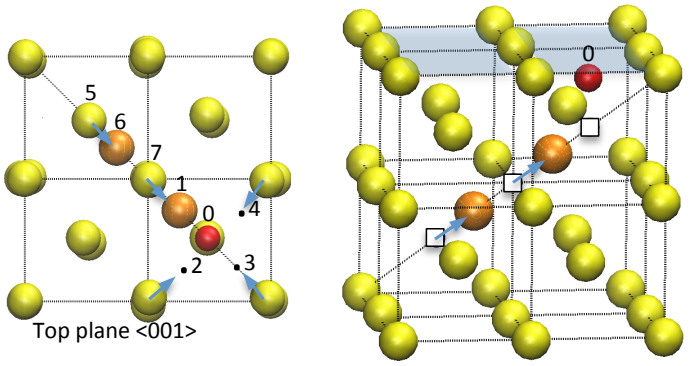

b) C jump after V jump

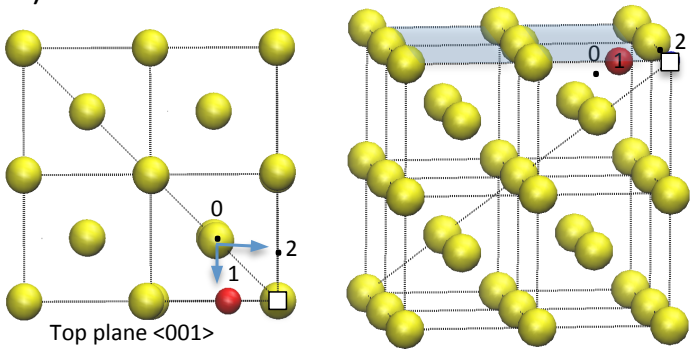

O.A. Restrepo, N. Mousseau, F. El-Mellouhi, O. Bouhali, M. Trochet, C. S. Becquart, Computational Materials Science **112**, Part A, 96-106 (2016).

C-substitutional in Fe

A complex diffusion:

C-interstitial diffusion barrier: 0.81 eV

The vacancy diffusion barrier: 0.64 eV

Vacancy-C bound state barrier: 1.5 eV

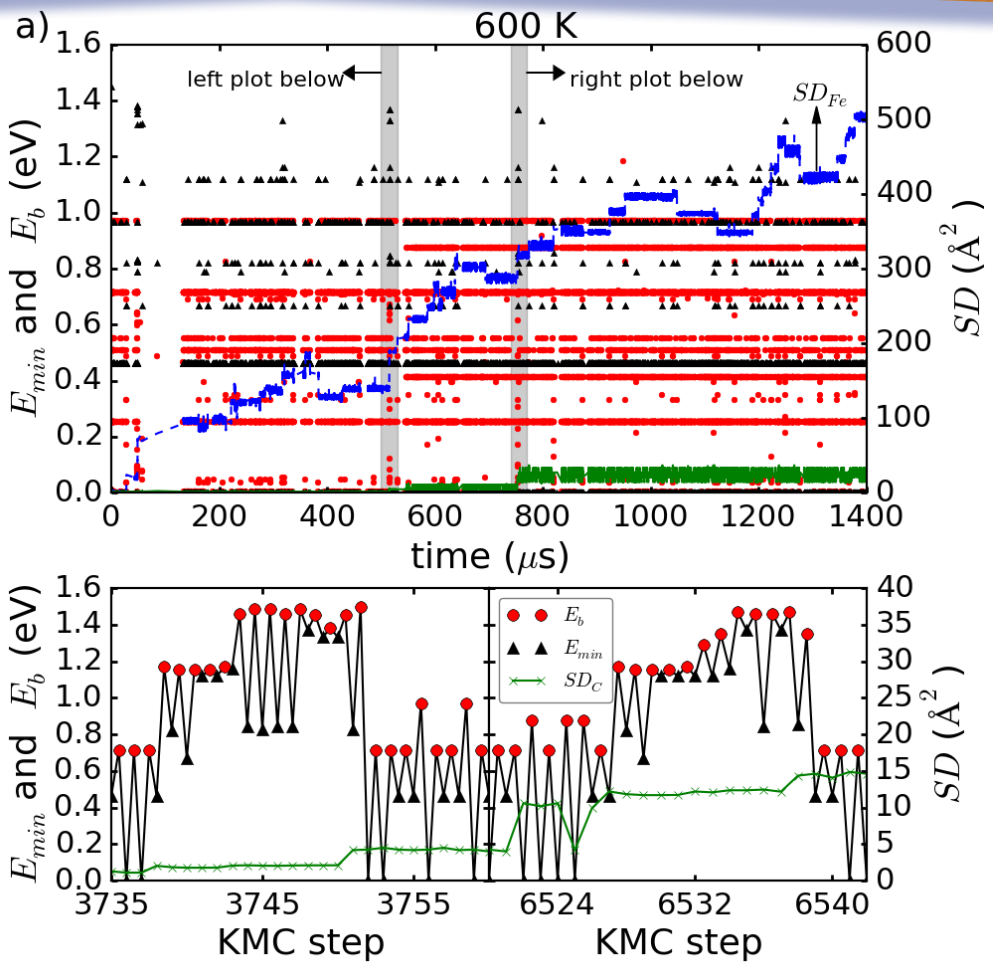

C diffusion at GB

For a long time, it was believed that GBs provide rapid pathways for impurities, particularly for C in bcc-metals.

This simple image was criticized recently by a number of groups who suggested that diffusion could be enhanced or reduced by the presence of these interfaces, and that their overall behavior was linked to free volume.

A. Oudriss, J. Creus, J. Bouhattate, E. Conforto, C. Berziou, C. Savall, X. Feaugas, Acta Mater, 60, 6814 (2012).

S. M. Teus, V.F. Mazanko, J.-M. Olive, V.G. Gavriljuk, Acta Mater. 69, 105 (2014).

Effects of Grain Boundaries

- For a long time, it was believed that GBs provide rapid pathways for impurities
- This simple image was criticized recently. It was suggested that diffusion could be enhanced or reduced by the presence of these interfaces, and that their overall behavior was linked to free volume.

See, for example: A. Oudriss et al. , Acta Mater, 60, 6814 (2012); S. M. Teus et al., Acta Mater. 69, 105 (2014).

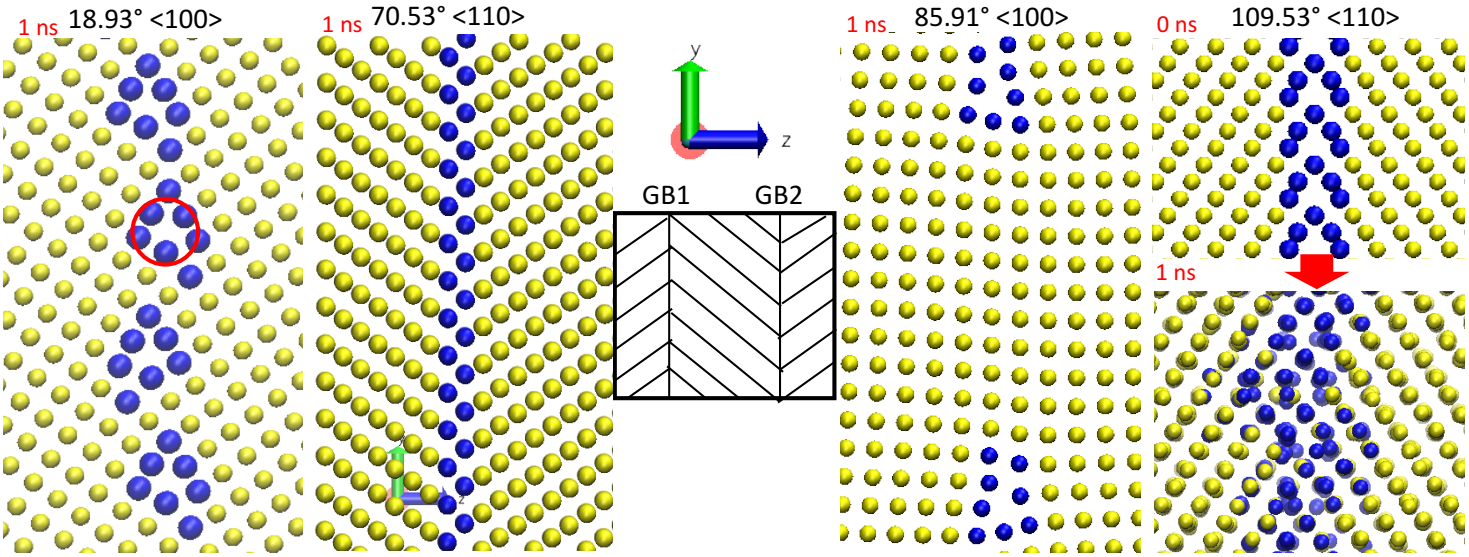

O.A. Restrepo, N. Mousseau, F. El-Mellouhi, O. Bouhali, C. S. Becquart, submitted.

Diffusion of Grain Boundaries

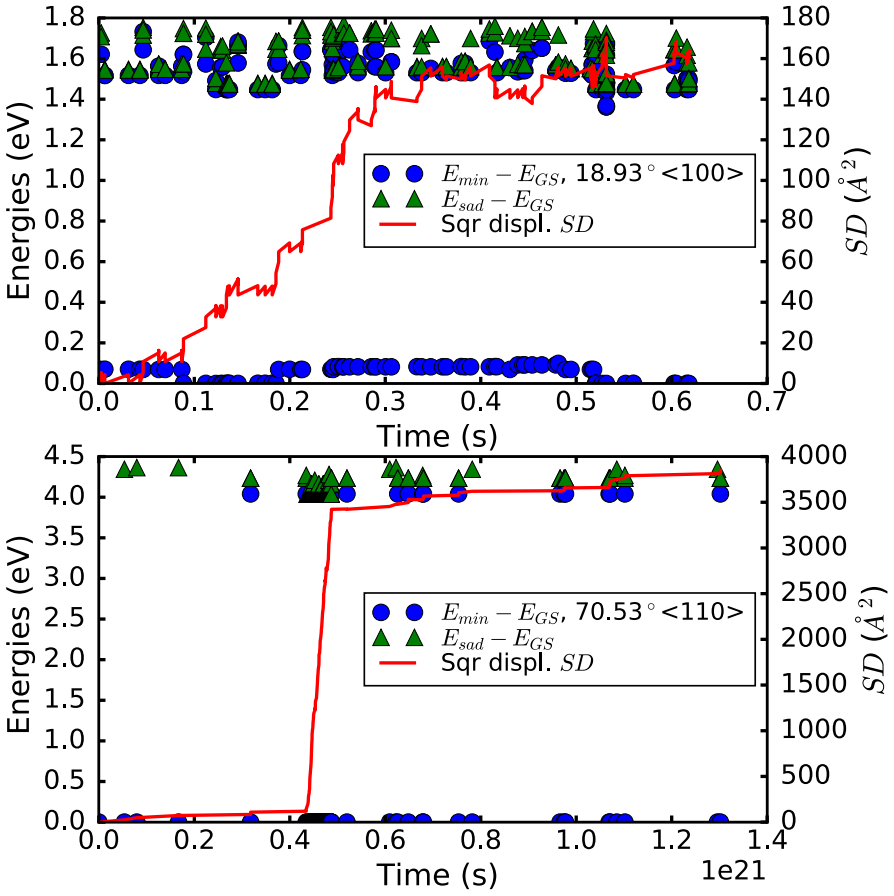

T=600 K

C diffusion at grain boundaries

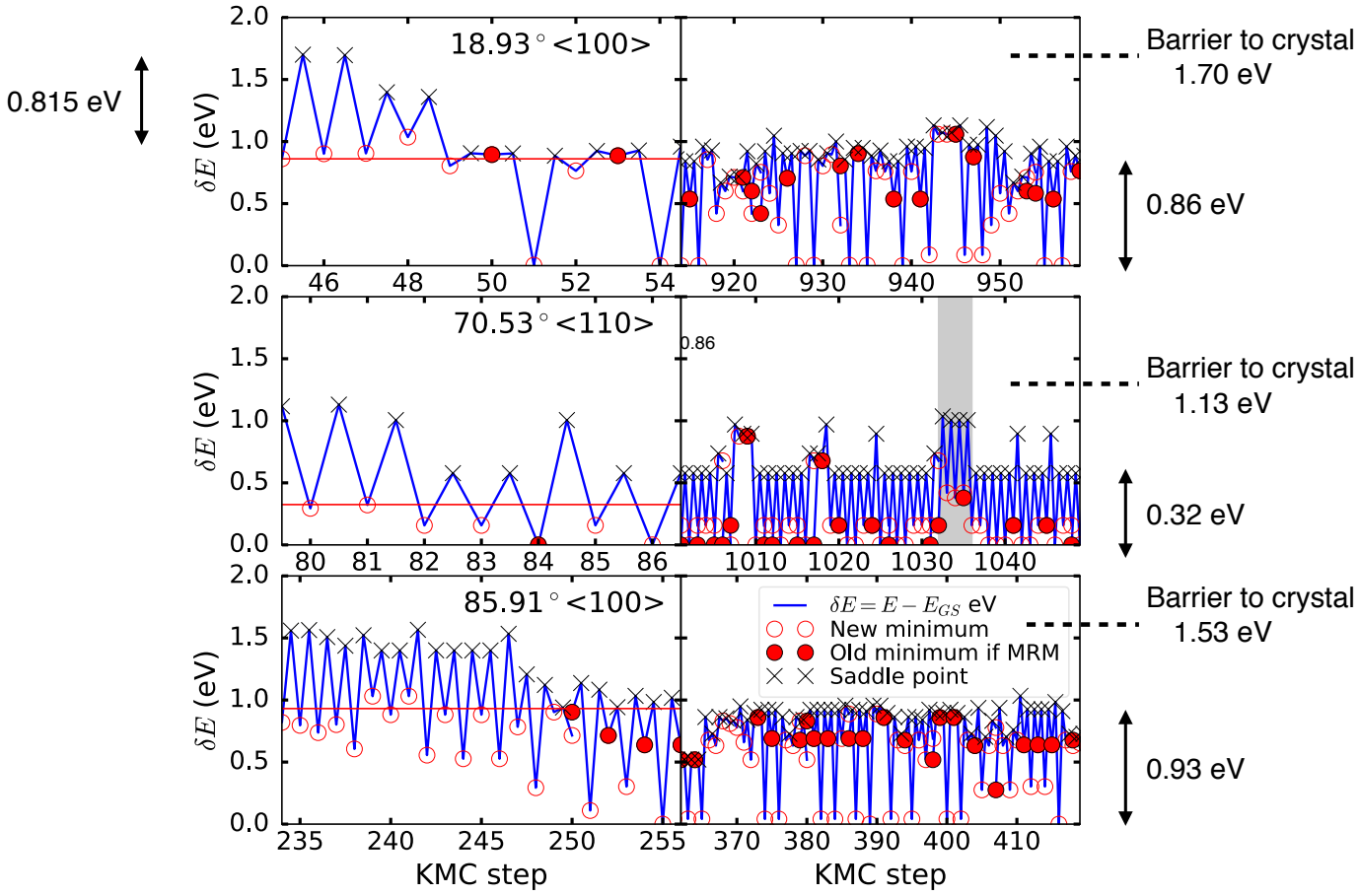

C diffusion at grain boundaries

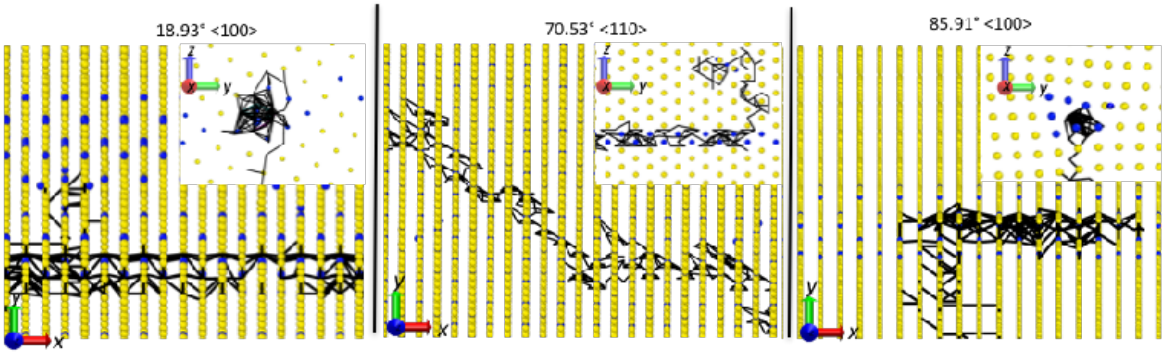

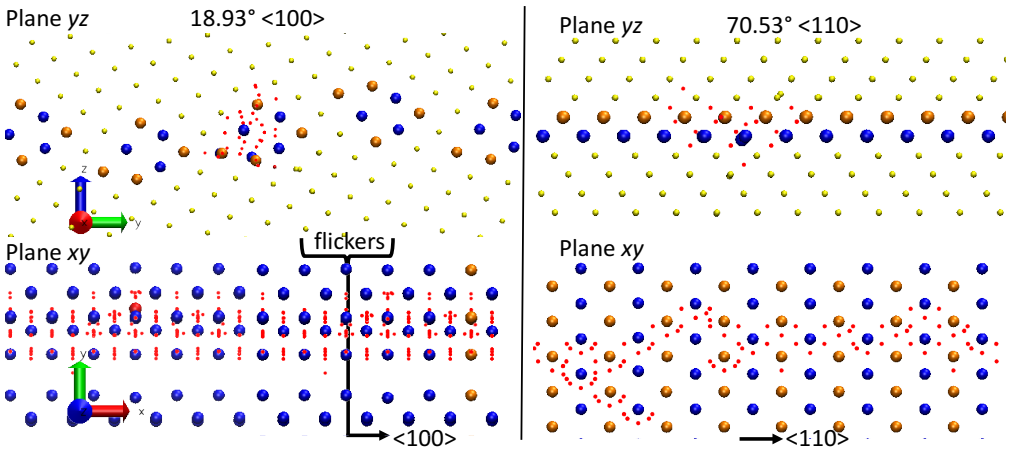

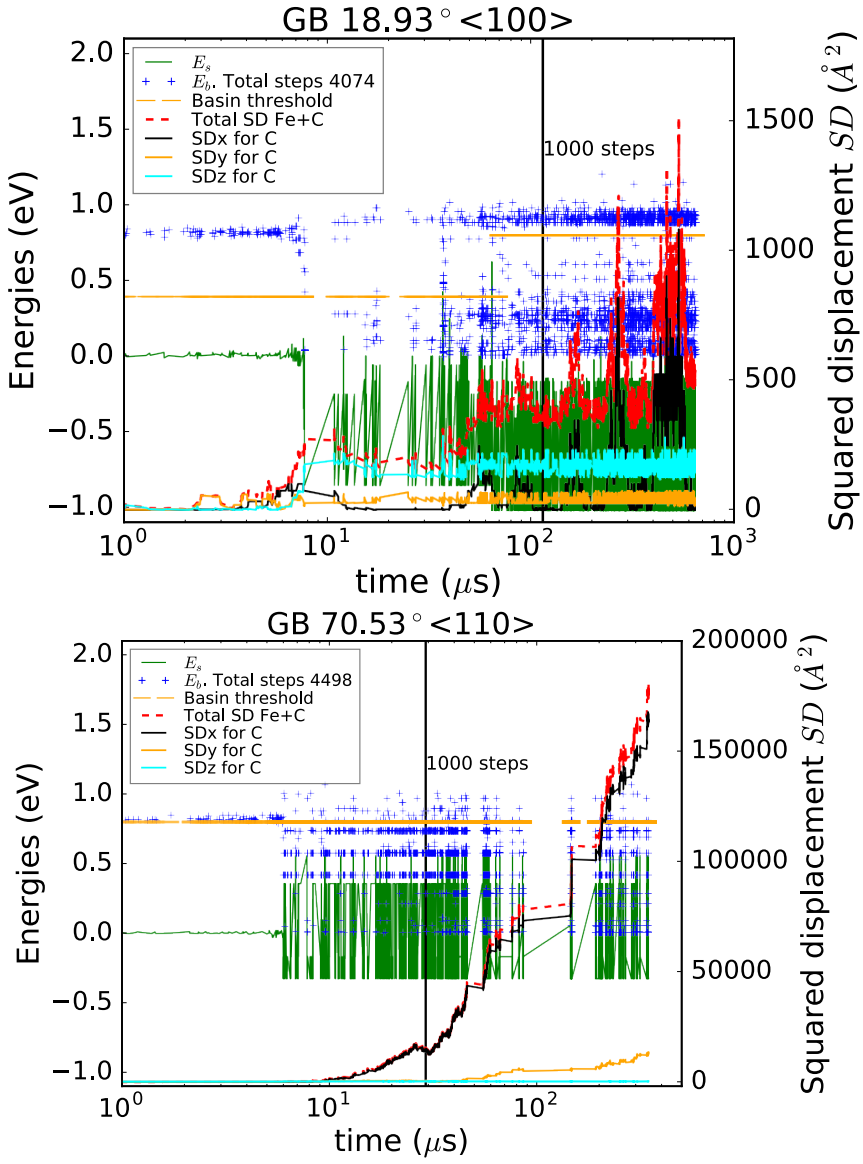
GB 18.93° <100>
E_s
E_b. Total steps 4074
Basin threshold
Total SD Fe+C
SDx for C
SDy for C
SDz for C
1000 steps
Energies (eV)
Squared displacement SD ($\AA^2$)
time (μs)
GB 70.53° <110>
E_s
E_b. Total steps 4498
Basin threshold
Total SD Fe+C
SDx for C
SDy for C
SDz for C
1000 steps
Energies (eV)
Squared displacement SD ($\AA^2$)
time (μs)

T=600 K

C diffusion at grain boundaries

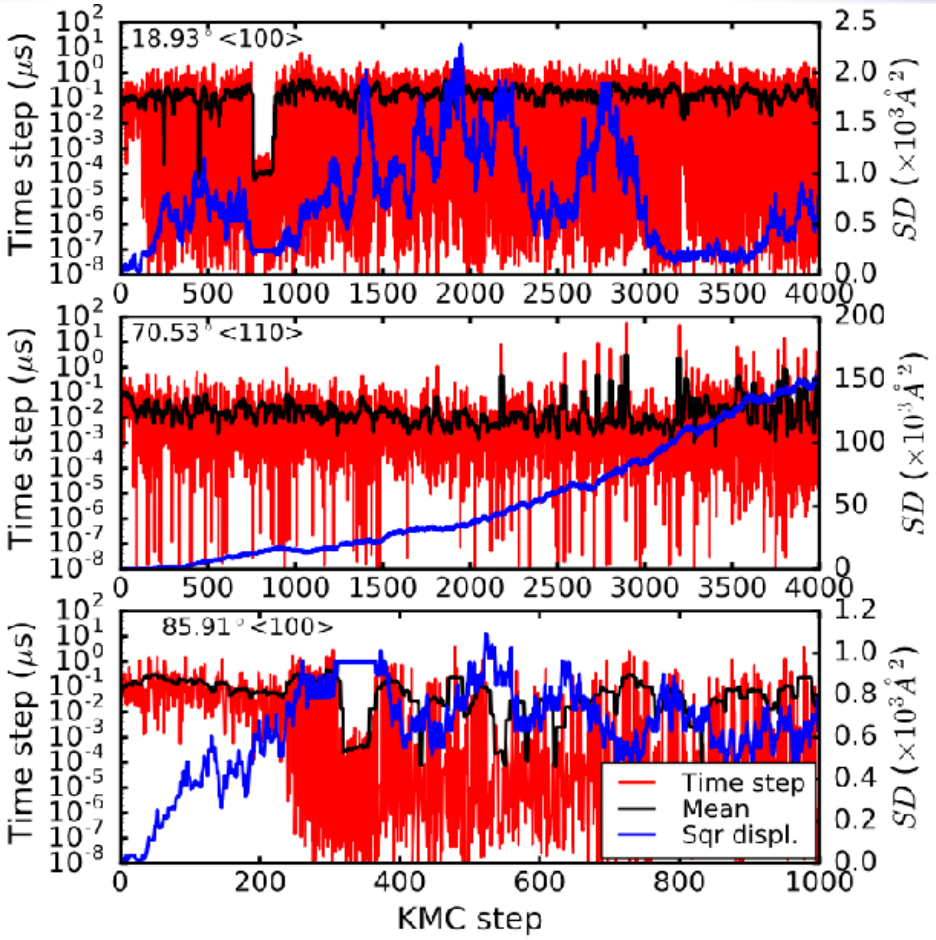

C diffusion at grain boundaries

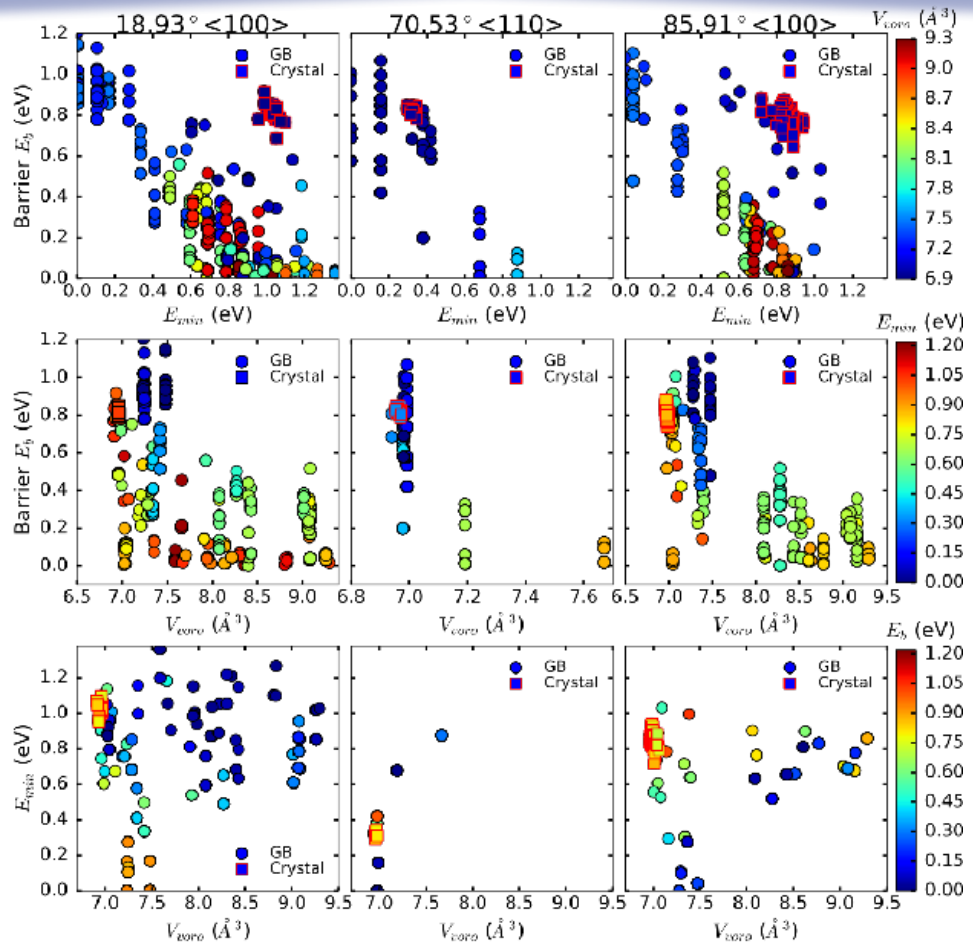

Conclusions- C diffusion at GB

- For the three stable GBs, C diffuses and remains largely trapped at the GBs, with energy gains ranging between 0.3 and 0.9 eV with respect to the bulk energy.
- Diffusion determined by the effective barriers between the lowest-energy states in the GB.
    - These can be either lower or higher than for bulk C diffusion, ranging from 0.5 to 1.2 eV depending on the GB.
    - Whether slower or faster than in the bulk, impurity diffusion takes place along the GB.
    - C paths can be unidimensional or two dimensional. More precisely diffusion takes place mostly along 1D channels for the 18.93° <100> and 85.91° <100> systems and it can explore the full 2D GB-plane for the 70.53° <110> GB.
- Contrary to what was proposed, the impurity diffusion barriers a**re not directly correlated with the available free volume**.

O.A. Restrepo, N. Mousseau, F. El-Mellouhi, O. Bouhali, C. S. Becquart, submitted.

Vacancies in Iron

Accumulation of point defects and their complexes in irradiated metals as studied by the use of positron annihilation spectroscopy

M. Eldrup and B.N. Singh, Journal of Nuclear Materials **323** (2003) 346–353

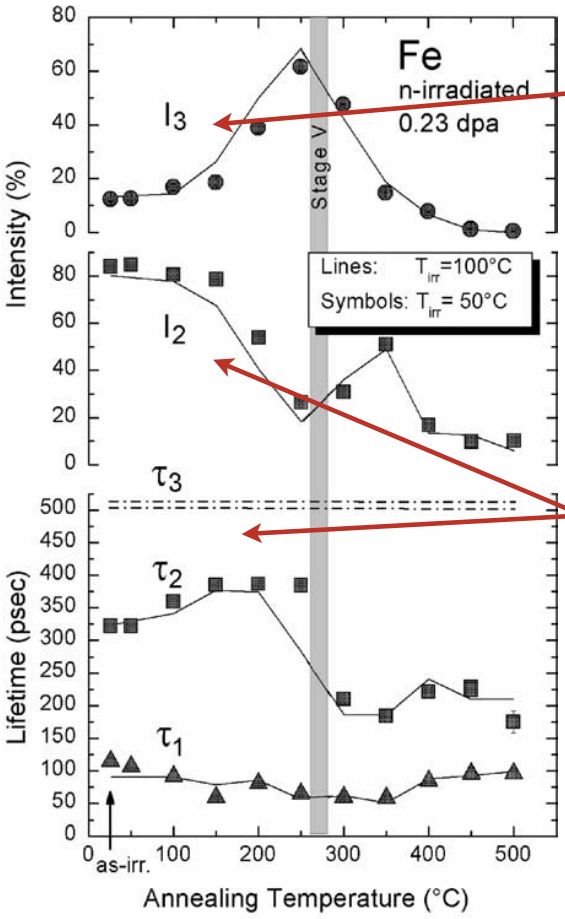

OUR APPROACH:

50 randomly placed vacancies in 2000-atom box;

Mendeleev Potential.

Vacancies in Iron

50 randomly placed vacancies in 2000-atom box; Mendeleev Potential.

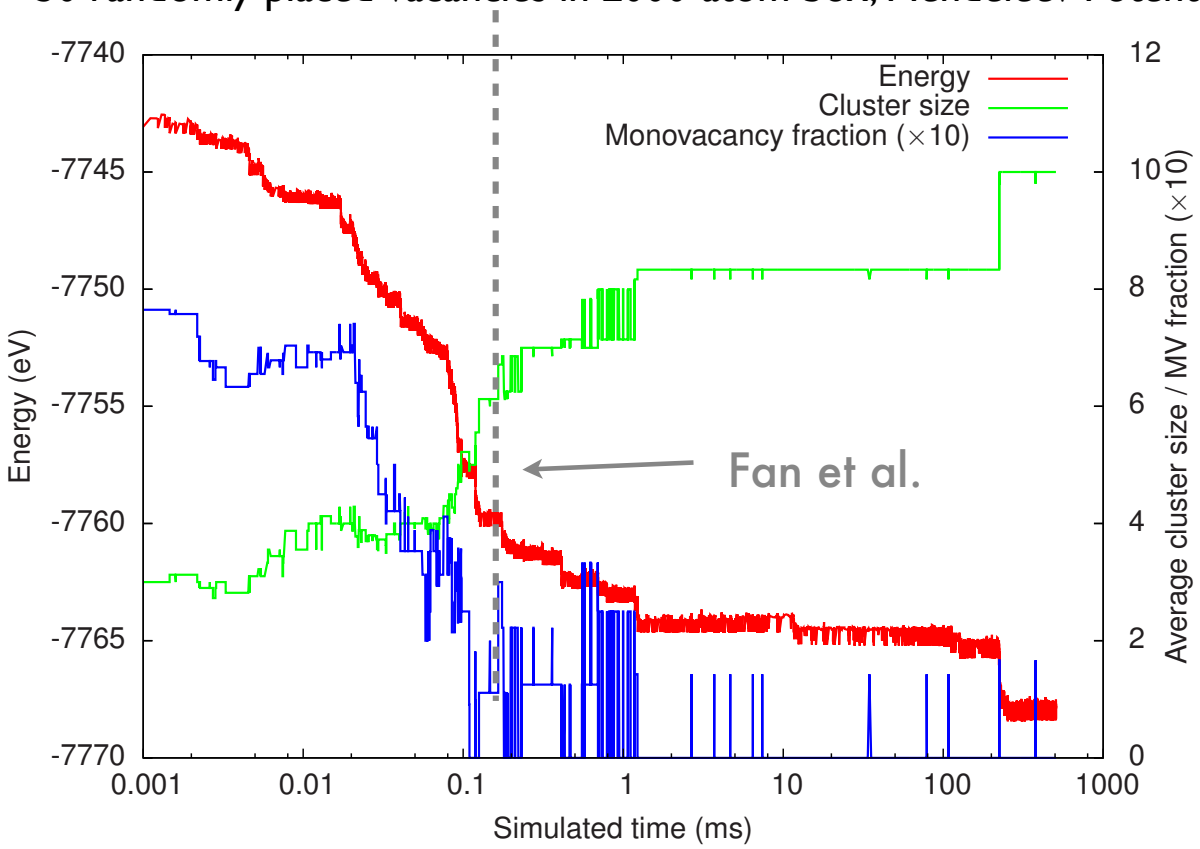

Brommer *et al.* PRL (2011); PRB (2014)

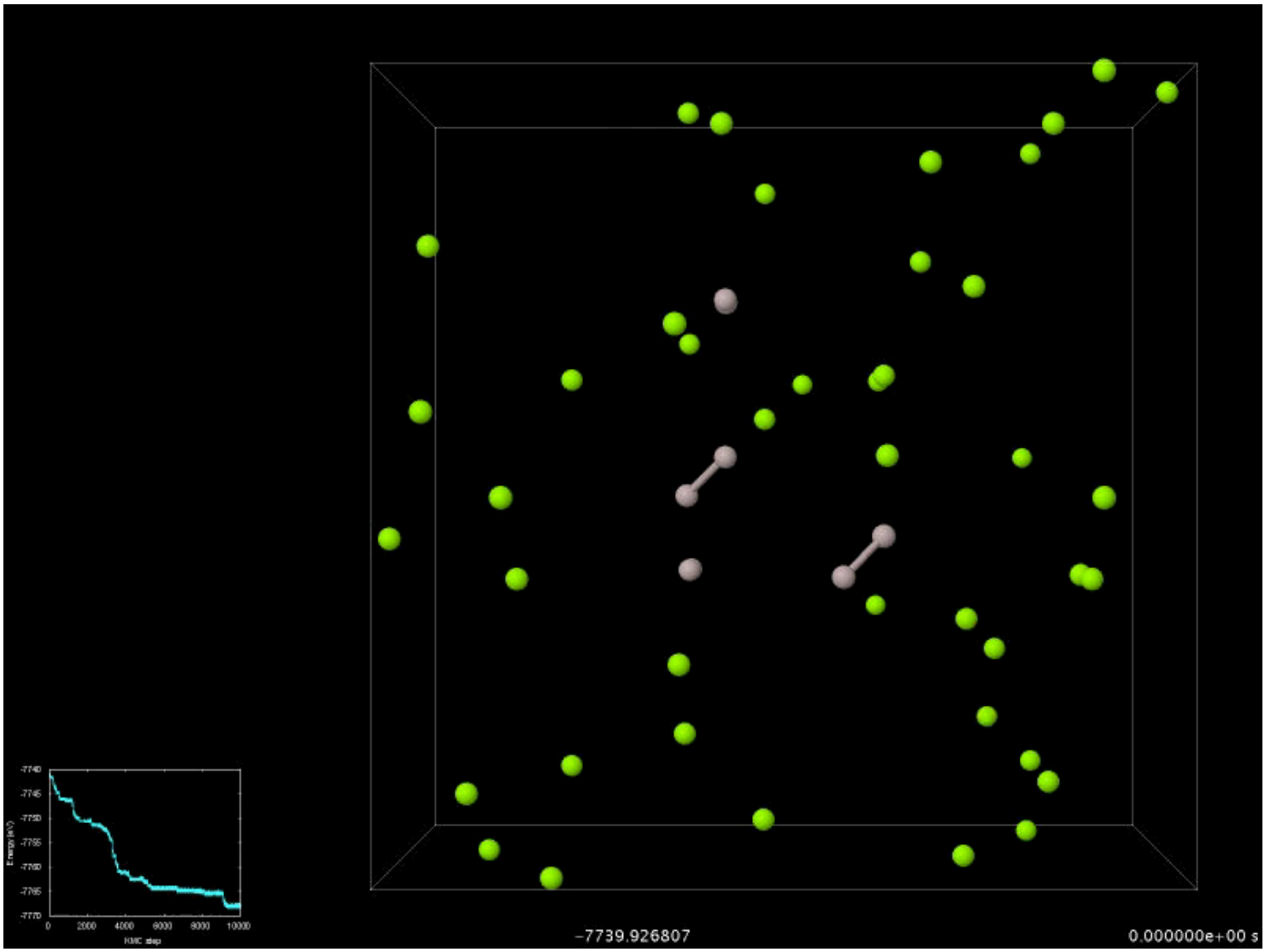
-7740
-7745
-7750
-7755
-7760
-7765
-7770
0
2000
4000
6000
8000
10000
HMC step
-7739.926807
0.000000e+00 s

CONCLUSIONS

- Kinetic ART is an efficient on-the-fly kinetic Monte-Carlo algorithm
- It uses a topological description for the classification of events; the flexibility of nauty allows us to take into account multiple components and more
- It defines two classes of events:
  - low-energy barriers that must be refined after each event
  - high-energy barriers which are treated as ensemble

- Kinetic ART is particularly useful for the study of diffusion in when strain effects are important or asymmetries prevent the use of standard KMC (e.g. presence of defects, interface, etc.).
- It is ideal for problems where
  - where the type of barriers evolves with time — self-organisation and aggregation phenomena
  - with complex environments - alloys, grain boundaries, disordered systems
- A number of details make the method efficient:
  - parallelization
  - recycling of low-energy barriers
  - handling of highly symmetric events
  - handling of blinkers
  - use of local forces for O(1) calculations

K-ART CODE

- available at normand.mousseau@umontreal.ca
- distributed freely/collaboration preferred for first project

THANK YOU